

Role of DPY-30 Proteins in Flagella

Radhika Gopal
Marquette University

Recommended Citation

Gopal, Radhika, "Role of DPY-30 Proteins in Flagella" (2010). *Dissertations (2009 -)*. Paper 63.
http://epublications.marquette.edu/dissertations_mu/63

ROLE OF DPY-30 PROTEINS IN FLAGELLA

by

Radhika Gopal M.Sc.

A Dissertation Submitted to the Faculty of
the Graduate School, Marquette University,
in Partial Fulfillment of the Requirements for the
Degree of Doctor of Philosophy

Milwaukee, Wisconsin

August 2010

ABSTRACT
ROLE OF DPY-30 PROTEINS IN FLAGELLA

RADHIKA GOPAL

MARQUETTE UNIVERSITY, 2010

Cilia and flagella are similar organelles found in eukaryotic cells. A microtubule-based axonemal cytoskeleton supports these organelles that project into the extracellular environment to detect various stimuli and propel fluid. These functions enable cells to sense and respond to the changing environment. Because of their importance, the fundamental mechanisms have been conserved throughout evolution. However, it remains largely unknown how axonemes are assembled and how the motility is regulated. This thesis investigated two molecules, RSP2 and RSP23, positioned in the axonemes within a T-shaped complex, the Radial Spoke (RS). Among several axonemal complexes, flagella lacking the evolutionarily conserved RS are paralyzed suggesting that this complex is crucial for motility. It was proposed that the RS transduces mechanical and chemical signals to regulate flagellar beating. These two molecules, RSP2 and RSP23, in *Chlamydomonas* bind the prototype calcium sensor, calmodulin. They also share a highly conserved DPY-30 domain that resembles the RIIa domain known for dimerization and targeting of cAMP-dependent protein kinase A to specific intracellular locations. Moreover, RSP2 links the head and stalk modules in the RS while RSP23 contains a Nucleoside Diphosphate Kinase (NDK) domain presumably for maintaining the equilibrium of nucleotide species. To reveal the mechanisms mediated by these molecules, mutants defective in these domains were generated. The calmodulin-binding region in RSP2, that is absent in mammalian homologs, is not required for the assembly of RS or the oscillatory beating. However, the motile mutants cannot maintain the typical helical trajectory when cells are exposed to bright light and glass barrier simultaneously. In contrast, mutants lacking the DPY-30 domain in RSP2 are paralyzed, despite the presence of all RSPs. Mutants expressing a fraction of RSP23 with inactive NDK activity generate shorter flagella with reduced amounts of RS. Together these results suggest that DPY-30 domains targets to key locations conserved molecular modules critical for flagellar elongation and motility and the diverged calmodulin-binding regions for steering the biflagellate. Models are proposed to illustrate the various roles of these molecular domains. These discoveries provide new insight on the extraordinary mechanisms in cilia and flagella.

ACKNOWLEDGEMENTS

Radhika Gopal M.Sc.

I would like to thank several people without whom this dissertation would not be possible.

First, I would like to thank my mentor Dr. Pinfen Yang for her support throughout the work that led to this dissertation. Her constant encouragement, motivation and advice helped me immensely. Critical thinking, vision and thinking ahead are just few of the many things I learnt from her. Her support guided me to make good decisions regarding my research project and future career. I will be forever thankful for the experience of working with her and learning from her.

I would like to thank all my committee members, Dr.Rosemary Stuart, Dr.Stephen Downs, Dr.Jane Dorweiler and Dr.Stephen Munroe. Their support and ideas were highly valuable throughout my work. They helped me see my project from a new point of view.

I am thankful to all the members in my lab, Anjali Gupta, Priyanka Sivadas, Stephanie Davis and Mei Wei. I would like to thank them for their friendship, support and critical evaluation of my work.

Last but not the least, I would like to thank my family members- my parents, my sister and my husband, Sujjahad. If not for their love and support, none of this would be a reality.

TABLE OF CONTENTS

ACKNOWLEDGMENTS	i
LIST OF TABLES	vi
LIST OF FIGURES	vii
LIST OF ABBREVIATIONS	ix
CHAPTER	
I INTRODUCTION	1
1.1 Role of Eukaryotic Cilia and Flagella	1
1.2 Structure and Assembly of Eukaryotic Flagella	3
1.3 Current Model of Flagellar Motility	6
1.4 <i>Chlamydomonas reinhardtii</i> as a Model System	7
1.5 Motility in <i>Chlamydomonas</i>	8
1.6 Calcium-mediated Modulation of Flagellar Motility	10
1.7 Biochemical Characterization of Radial Spoke Complex	12
1.8 Assembly of the RS Complex	14
1.9 Goals of the Dissertation	16
II MATERIALS AND METHODS	17
2.1 Strains and Culture Conditions	17
2.2 Sequence Analysis	17
2.2 Molecular Biology	18
2.2.1 Cloning	18
a) Generation of Bacterial Constructs	18
i) RSP2 Constructs	18
ii) RSP23 Constructs	18
b) Generation of Constructs for Expression of RSP2 in <i>Chlamydomonas</i>	19
i) Δ DPY-30	19
ii) Δ CT-Tag	19
iii) Δ CT	20
iv) RSP2 ₁₋₁₂₀	20

v)	CaMB*	20
c)	Generation of Constructs for the Expression of RSP23 in <i>Chlamydomonas</i>	22
2.2.2	Generation of RS Mutant Strains	22
2.3	Screening of Transformants	23
2.3.1	96-well Methods for RSP2 Transformants	23
2.3.2	Flagella Prep for RSP23 Transformants	24
2.4	Biochemistry	24
2.4.1	Axoneme Preparation	24
2.4.2	Isolation of RS Complex by Sucrose Gradient Fractionation	25
2.4.3	Calmodulin Affinity Purification	25
2.4.4	SDS-PAGE	26
2.4.5	Protein Gel Transfer	26
2.4.6	Western Blot Analysis	27
2.4.7	Western Blot for Calmodulin	27
2.5	Motility Analyses	28
III	THE ROLE OF THE EVOLUTIONARILY CONSERVED N-TERMINUS OF RSP2	32
3.1	Introduction	32
3.2	Results	33
3.2.1	Sequence Analysis of the Conserved RSP2 N-terminus	33
3.2.2	DPY-30 Domain of RSP2 is Crucial for Flagellar Motility	40
3.2.3	The Conserved N-terminus of RSP2 is Sufficient for Motility	44
3.2.4	Radial Spoke Composition in RSP2 Mutants	44
3.2.5	Stability of the Radial Spoke Complex	47
3.3	Discussion	49
3.3.1	The Conserved N-terminus of RSP2 is Sufficient to Restore Motility	49
3.3.2	DPY-30 Domain of RSP2 is Crucial for Oscillatory Beating	49
3.3.3	KI-Sensitivity of the Restored RS in the Two RSP2 Truncation Mutants	50

IV THE ROLE OF THE CALMODULIN-BINDING C-TERMINUS IN RSP2	52
4.1 Introduction	52
4.2 Results	55
4.2.1 C-terminus of RSP2 Maintains Helical Trajectory of Cells in Bright Light	55
4.2.2 Irregular Trajectory of Mutants is not Due to Impaired Photoaccumulation	58
4.2.3 Irregular Trajectory of 1-120 Cells is Dependent on Direction of Illumination	60
4.2.4 Light-Induced Irregular Swimming of Mutant Cells is Calcium-dependent	62
4.2.5 Perturbation in Calmodulin-binding Properties of RSP2 Leads to Irregular trajectory	64
4.2.6 Persistent Light Response of RSP2 Calmodulin-binding Mutants	66
4.2.7 1-120 Strain Does Not Bind Calmodulin	69
4.2.8 Motility and Assembly Deficiencies in RSP2 C-terminus Mutants	71
4.3 Discussion	74
4.3.1 C-terminus of RSP2 Mediates of the Steering of Cells Under Conflicting Signals	74
V ROLE OF NDK DOMAIN IN RSP23	77
5.1 Introduction	77
5.2 Results	83
5.2.1 NDK Mutants are Defective in Flagellar Assembly	84
5.2.3 NDK Mutants are Defective in Radial Spoke Proteins	85
5.3 Discussion	89
VI DISCUSSION	91
6.1 The Conserved RSP2 N-terminus as a Bivalent Structural Linker	91
6.2 The C-terminus of RSP2 with the CaMB Region Modulates	93

Spoke Head and Photoresponse	
6.3 NDK Activity of RSP23 is Important for Assembly of RS Complex and Flagella	98
6.4 The Role of RIIa Superfamily	99
6.5 Key Findings and Significance	103
REFERENCES	105

LIST OF TABLES

Table I	List of all radial spoke proteins and their location in the radial spoke complex	13
Table II	Sequences of Primers Used	29
Table III	Antibodies Used, their Host, Respective Antigens and Source Reference	31
Table IV	RIIa Domain Containing Proteins in Humans	37
Table V	DPY-30 Domain Containing Proteins in Humans	38
Table VI	Light-Induced Irregular Movement of RSP2 ₁₋₁₂₀ Cells is Calcium-Dependent	63

LIST OF FIGURES

Figure 1-1	Ultrastructure of 9+2 Cilia and Flagella	5
Figure 1-2	Helical Swimming in <i>Chlamydomonas</i>	9
Figure 1-3	Schematic Showing RS-CP Interaction and Predicted Positions of RSP2, 23 and 16 in the Neck region	15
Figure 2-1	Creation of RSP2 Deletion and Mutation Constructs	21
Figure 3-1	DPY-30 Domain in RSPs	35
Figure 3-2	Comparison of the N-terminal 120 a.a. in <i>Chlamydomonas</i> RSP2 and Human DYDC2	39
Figure 3-3	RSP2 Constructs	41
Figure 3-4	DPY-30 Domain of RSP2 is Crucial for Motility	43
Figure 3-5	RSP2 Deletion Mutants Restore Biochemical Deficiencies of RS Complex	46
Figure 3-6	DPY-30 Domain is Required for the Stability of RS Complex and Integrity of the Spoke Base	48
Figure 4-1	Calmodulin Binding Sites in RSP2	54
Figure 4-2	Mutant Lacking C-terminus of RSP2 Displays Irregular Swimming Path Under Increased Light Intensities	56
Figure 4-3	Irregular Trajectory of Mutant cells was Reversible and Dependent on Illumination Levels	57
Figure 4-4	1-120 and Control Cells Photoaccumulate in a Similar Manner	59
Figure 4-5	The Irregular Trajectory is Related to the Direction of Light	61
Figure 4-6	Mutants that Express Full-Length RSP2 with a Defective CaMB motif also displayed the Light-Induced Irregular Trajectory	65
Figure 4-7	Orientation of Cells and Asynchrony Flagella under Conflicting Stimuli	68
Figure 4-8	Altered CaMB Affinities Due to RSP2 Mutations	70
Figure 4-9	Altered Assembly of Spoke Head Proteins in RSP2 C-terminus Mutants	73
Figure 4-10	Schematic Depicts the Movement of Control and RSP2 Mutants From High Speed Video Microscopy Images	76

Figure 5-1	Molecular Domains, Catalytic Mechanisms and Mutation Constructs of NDK (RSP23)	82
Figure 5-2	Representative Western Blots of Flagella from Clones Transformed with Control or Mutant NDK Constructs	86
Figure 5-3	Inactive NDK Mutants have Shorter Flagella	87
Figure 5-4	Radial Spoke Complex is Less Abundant in the Axonemes of Inactive NDK Mutants	88
Figure 6-1	Model Illustrating Role of RSP2 Conserved Region in Assembly of RS and motility	92
Figure 6-2	Model Elucidating Role of CaMB Domain of RSP2	97

LIST OF ABBREVIATIONS

2D	Two Dimensional
ADK	Adenylate Kinase
ATP	Adenosine TriPhosphate
ATPase	Adenosine TriPhosphatase
BLAST	Basic Local Alignment Search Tool
BSA	Bovine Serum Albumin
C	Control
CaM	Calmodulin
CaMB	Calmodulin-Binding
CCD	Charge-Coupled Device
Cont	Control
CP	Central Pair
D	Dim
D/D	Dimerization and Docking
DYDC1/2	DPY-30 Domain Containing 1/2
EM	Electron Microscopy
GTP	Guanosine TriPhosphate
HMT	Histone Methyl Transferase
HRP	Horse Radish Peroxidase
HSP40	Heat Shock Protein 40
HSP70	Heat Shock Protein 70
IC	Intermediate Chain
IDA	Inner Dynein Arm
IFT	IntraFlagellar Transport
KI	Potassium Iodide
LC	Light Chain
M	Molar
MBP	Maltose Binding Protein
N	Normal
NDK	Nucleoside Diphosphate Kinase
NDP	Nucleoside DiPhosphate
NTP	Nucleoside TriPhosphate
ODA	Outer Dynein Arm
<i>pf</i>	paralyzed flagella
PKA	Protein Kinase A
PKD	Polycystic Kidney Disease
PMM	Paromomycin
RS	Radial Spoke
RSP	Radial Spoke Protein

SMART	Simple Modular Architecture ResearchTool
TAP	Tris Acetate Phosphate
WT	Wild Type

CHAPTER I. INTRODUCTION

1.1 Role of Eukaryotic Cilia and Flagella

Cilia and flagella are similar organelles projecting from the cell surface into extracellular space. Most vertebrate cells have either of these organelles to perform crucial functions. The terms cilia and flagella are used interchangeably in this thesis.

These organelles diverge structurally and functionally according to the cell types (Ginger et al., 2008). In general, they function like cellular antennae and transduce extracellular signals to orchestrate a wide range of reactions. For example, the cilium on the kidney epithelial cells detects fluid flowing through the renal tubules. The signaling regulates proliferation, polarity and apoptosis of kidney cells (Wilson and Goilav, 2007).

Some of these organelles are equipped with additional machinery to sweep fluids surrounding the cells (Satir and Sleight, 1990). This movement is crucial for the normal function of vital organs. For instance, epithelium of the mammalian respiratory system, reproductive tract and central nervous system employ tufts of cilia to propel mucous or fluid on the surface. A single flagellum propels sperm towards oocytes during fertilization (Kaupp et al., 2008). Moreover, nodal cilia generate directional flow that is instrumental in the establishment of left-right asymmetry during early embryonic development (Nonaka et al., 2002).

Defects in these diverged organelles can result in a wide range of symptoms collectively referred to as ciliopathies (Badano et al., 2006). The most extensively studied is Polycystic Kidney Disease (PKD). Defective signaling in kidney cilia results in uncontrolled proliferation of epithelial cells leading to multiple enlarged cysts that

replace the normal tissues (Wilson and Goilav, 2007). Some of these patients with defective cilia exhibit retinal degeneration, hypertension and diabetes (Afzelius, 2004). These disparate symptoms are attributed to the defective sensory cilium. On the other hand, deficiencies in motile cilia defects are manifested as chronic respiratory tract infections, infertility, hydrocephaly and situs inversus. These symptoms are collectively referred to as Kartagener's syndrome or primary ciliary dyskinesia (Afzelius, 1976). Genetic analyses indicate that ciliopathies are polygenic. However, only a few causative genes have been identified and the molecular mechanisms are not wholly understood.

Cilia and flagella are also commonly found in simple organisms, such as *Paramecium*, *Tetrahymena* and *Chlamydomonas*, the model organism used in this study. These protists employ motile cilia and flagella to swim towards favored environments, escape from predators, capture prey, ingest food and mate. These behaviors enable the species to survive in the changing environment. Parasitic trypanosomes that cause sleeping sickness require flagellar motility to establish infection in the host suggesting the importance of this organelle. All these examples suggest that the key features of these organelles have been preserved throughout evolution.

1.2 Structure and Assembly of Eukaryotic Flagella

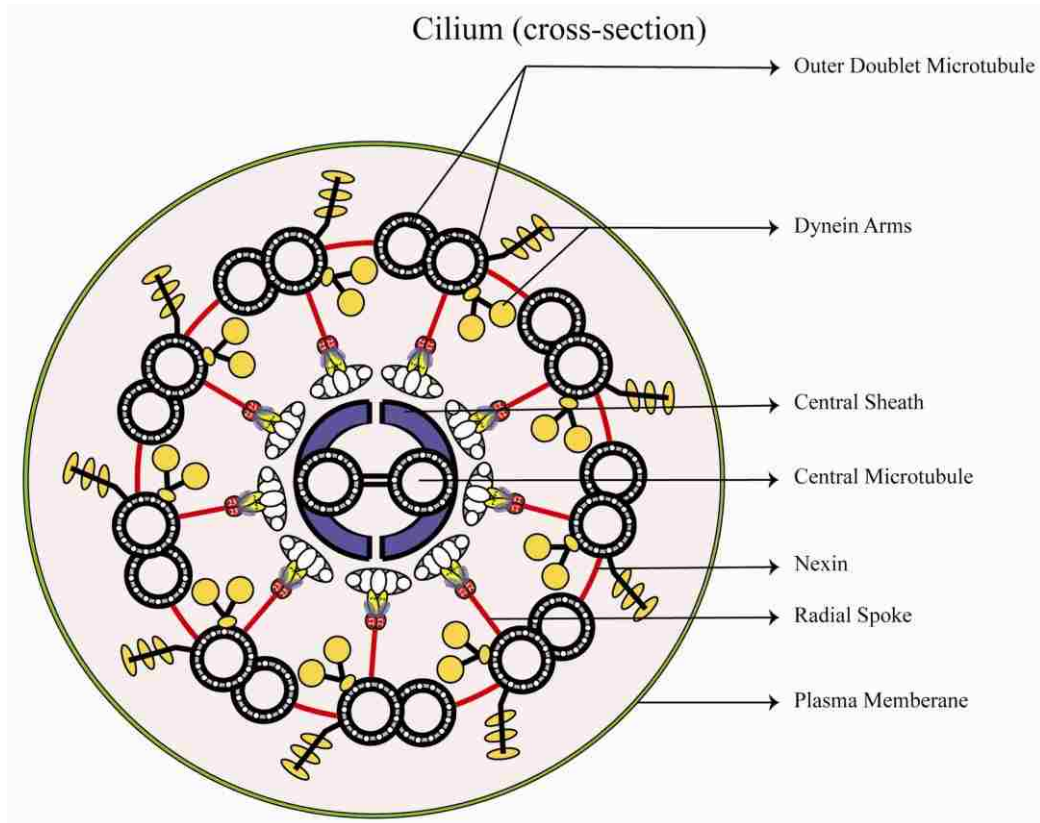
Cilia and flagella are supported by a microtubule based cytoskeleton known as the axoneme. There are two types of axonemes. Sensory cilia usually contain the 9+0 format with 9 outer doublets arranged in a circle. In contrast, axonemes in motile cilia are much more complicated. Motile cilia adopt an evolutionarily conserved 9+2 axoneme. The 9 outer doublet microtubules surround the Central Pair (CP) apparatus that is comprised of 2 singlet microtubules and associated projections (Figure 1-1A). Dynein arms anchor to the 'A' tubule of outer doublets via a base and project its motor domains towards the adjacent outer doublet. Upon hydrolysis of adenosine triphosphate (ATP), the motor domain of dynein translocates toward the minus end of the microtubule, leading to the interdoublet sliding. This sliding is ultimately converted into a bend and oscillatory beating. The T-shaped Radial Spoke (RS) complex also anchors to the A-tubule of outer doublets via a thin stalk while the bulbous spoke head projects towards the CP (Figure 1-1A). As shown by Electron Microscopy (EM) of longitudinal sections, RS are present as doublets or triplets every 96-nm. This arrangement maintains a right-handed helix along the length of the axoneme (Goodenough and Heuser, 1985).

Contrary to the dynein arms, the role and mechanism of CP and RS are less characterized. It is postulated that these two structural complexes function as a control system crucial for the oscillatory beating (Huang et al., 1982). Mutant organelles defective in either of these structures are paralyzed despite the presence of dynein arms. Their importance explains the preservation of the 9+2 axoneme throughout evolution.

Most of the axonemal proteins function as macromolecular complexes. Assembly of hundreds of distinct proteins into axonemes entails elaborate processes. Since flagella

lack the machinery for protein synthesis, complex mechanisms exist to coordinate processes from synthesis in the cell body up to assembly in flagella. Axonemal proteins are synthesized in the cell body and assembled as precursor complexes (Qin et al., 2004). These complexes are then transported into the flagella by kinesin-driven intraflagellar transport into the flagellar compartment (Kozminski et al., 1993; Cole et al., 1998). Localization studies using antibodies against Radial Spoke Proteins (RSP) and labeled tubulin have shown that RS is transported to the tip, the distal end of the flagella, to be assembled into axonemes (Johnson and Rosenbaum, 1992). The prepackaging of individual components into precursor particles is presumed to ensure coordinated transport and assembly.

A



B

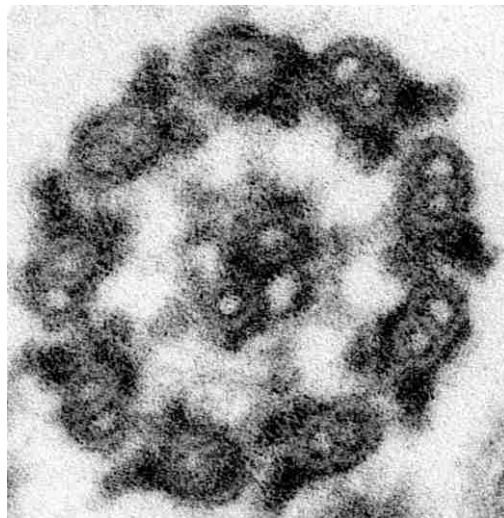


Figure 1-1: Ultrastructure of 9+2 Cilia and Flagella

A) Schematic of the cross section of a cilium showing the 9+2 axonemes inside with 9 outer doublets, central pair and T-shaped radial spokes. The dynein arms are anchored on the outer doublet B) EM section of the *Chlamydomonas* flagella showing the 9 outer doublet rings and associated structures.

1.3 Current Model of Flagellar Motility

The oscillatory beating of flagella is powered by hundreds of dynein motors. Dynein arms are distributed around the circumference and along the length of the axonemes. It is well recognized that if all dynein arms activate at once, the flagellum will become rigid. Conversely, the flagellum would be flaccid, if all dynein arms were inactive. Dynein motors must be activated in a sequential manner to coordinate oscillatory beating with rhythmic bend initiation and propagation.

RS, which is positioned between CP and dynein arms, appears to play a central role in controlling dynein activity. Studies using cilia from *Paramecium* and many other organisms revealed that the CP rotates within the nine doublet microtubules (Omoto and Kung, 1979; Omoto et al., 1999). It was proposed that the rotating CP makes periodic contacts with the RS, which in turn transduces mechanical signals (like force or tension) to activate dynein arms sequentially. EM of longitudinal sections of mussel gill cilia showed that the RS tilts relative to outer doublets and CP only at the bend. This observation led to the conclusion that RS undergoes cycles of attachment and detachment against the CP projections (Warner and Satir, 1974).

In addition, functional studies with microtubule sliding assays suggest that RS controls different subsets of dyneins via a network of kinases and phosphatases that convert second messenger signaling to changes in flagellar beating (Porter and Sale, 2000).

Despite the predicted roles of RS in motility control, the model cannot yet explain how these organelles beat at a high frequency with a sophisticated waveform and how second messengers like calcium modulate motility. In addition, the entire process leading

to the assembly of RS during flagella elongation is only partially understood. These questions about RS are fundamental in explaining how cilia and flagella assemble and beat. Because of the complexity of these mechanisms, the well characterized *Chlamydomonas* RS becomes an ideal system to address these long-standing questions.

1.4 *Chlamydomonas reinhardtii* as a Model System

Many studies on flagellar motility use the unicellular green algae *Chlamydomonas* (Division: Chlorophyta). Cells in this genus are biflagellate and motile. They can survive in a broad spectrum of environments ranging from alpine snow, soil, fresh water and oceans. The most widely used laboratory species is *Chlamydomonas reinhardtii*. This species grows readily on simple medium of inorganic salts supplemented with light for photosynthesis.

C. reinhardtii is an ideal model system for studying cilia and flagella because of a number of experimental advantages. It has a defined sexual cycle that can be manipulated under laboratory conditions. The most important benefit is the ease of genetic manipulations because of a haploid genome. Unlike many other simple organisms, flagella are not essential for the viability and growth of *Chlamydomonas*. This makes it possible to isolate numerous mutants exhibiting various flagellar phenotypes or paralyzed flagella (*pf*). Due to the evolutionarily conserved axonemal structure, the discovery of *Chlamydomonas* genes has become a major way to identify candidate genes involved in human diseases caused by defective cilia and flagella. Completion of the genome and flagella proteome projects has enhanced the utility of *Chlamydomonas* as a powerful model system (Pazour et al., 2005; Merchant et al., 2007). This combination of flagellar

mutants, proteomics, genetics and genome makes *C. reinhardtii* an ideal model system for the study of cilia and flagella.

1.5 Motility in *Chlamydomonas*

Chlamydomonas flagella beat with breast-stroke like waveform at a frequency of ~ 60 Hz. Each beat is divided into a power stroke and a recovery stroke (Figure 1-3; Brokaw 1982; Brokaw and Luck, 1983; Ruffer and Nultsch, 1985). During the “power” stroke, the flagella beat backwards remaining relatively straight and bending mostly at the base. In the “recovery” stroke, flagella are brought back to the initial position by a bend propagating from the base to the tip. The power stroke propels cells to move forward while the recovery stroke leads to a weaker backward motion. These two strokes overlap each other: the recovery stroke of the previous phase still propagates along the flagellum at the beginning of the next effective stroke. The velocity of swimming cells is mostly between 100-200 $\mu\text{m}/\text{sec}$.

Like most ciliates and flagellates, *Chlamydomonas* cells swim along a helical trajectory (Figure 1-3; Ruffer and Nultsch, 1985). In order for the biflagellate cell to swim in a helical path, the two beating flagella must generate unequal force and rotate the cell body (Ruffer and Nultsch, 1985). Studies using cell models have led to the conclusion that the outward directed flagellum occasionally beats faster than the other resulting in a helical swimming path (Kamiya and Witman, 1984).



Figure 1-2. Helical Swimming in *Chlamydomonas*.

Low speed video microscopy recording of WT *Chlamydomonas* cells revealed the helical swimming path of the cell. The cell was selected and tracked for 100 frames using Metamorph Image Analysis Software.

1.6 Calcium-Mediated Modulation of Flagellar Motility

It is speculated that the helical path allows cells to orient themselves to external stimuli by aligning the axis of their helical trajectory to the stimulus (Crenshaw, 1993; Friedrich and Julicher, 2007). The helical path especially enables *Chlamydomonas* cells to scan the environment using a structure known as the eyespot which is positioned around the equator. Exposure of the eyespot vertically to light excites the embedded photoreceptors, leading to membrane depolarization and transient opening of Ca^{2+} channels that are distributed on the flagellar membrane. This increase in intraflagellar Ca^{2+} triggers a change in flagellar beat. As two flagella are positioned cis and trans with respect to the eyespot, they are affected differentially leading to changes in flagellar bending, swimming direction and motility.

Depending on the intensity and wavelength of light, *Chlamydomonas* generates two different responses. The first is phototaxis which enables cells to turn towards or away from light. The other response is called photoshock. This occurs when cells respond to an intense pulse of light or mechanical stimulation. The forward movement of flagella stops followed by a backward movement with an undulatory symmetric bend like sperm flagella (Schmidt and Eckert, 1976; Hyams and Borisy, 1978; Bessen et al., 1980).

These two photoresponses are induced by calcium although at different concentrations. The intracellular calcium is maintained at around 10^{-8} M, ~1000 fold lower than the extracellular calcium concentration. In vitro studies suggest that phototaxis is induced by 10 fold changes in calcium concentration while calcium surges during photoshock exceeds 10^{-5} M (Kamiya and Witman, 1984). The rising calcium concentration results in a switch from forward swimming with asymmetric waveform, to

quiescence and then to backward swimming with symmetric waveform. Recent studies show that a voltage-gated calcium channel enriched near the flagellar tip may be involved in this motility switch during photoshock or mechanoshock responses (Fujiu et al., 2009). In addition, increased calcium concentrations can also elevate beat frequency (Smyth and Berg, 1982; Wakabayashi et al., 2009). How calcium changes these behaviors remains unknown.

Since these calcium-induced changes were observed in isolated demembrated axonemes and demembrated cell models, it was concluded that the calcium sensor is built into the axoneme (Bessen et al., 1980; Kamiya and Witman, 1984). Consistently, proteomics and cloning have discovered many calcium- and Calmodulin-Binding (CaMB) proteins in axonemes. Among them, Calmodulin (CaM) is highly abundant (Witman and Minervini, 1982). Many proteins that are unable to bind calcium bind CaM and use it as a calcium sensor and signal transducer. CaM changes conformation upon binding to calcium. This alters interactions between CaM and its binding partners.

A fraction of CaM is constitutively associated with the RS and CP complexes in *Chlamydomonas* flagella (Yang et al., 2001; Wargo et al., 2005). These two complexes are implicated in several motility changes induced by calcium, such as the calcium-dependent waveform switch and regulation of dynein motors (Brokaw et al., 1982; Dymek and Smith, 2007; Smith and Yang, 2004).

1.7 Biochemical Characterization of RS Complex (Table for RS members)

Studies of several RS mutants identified crucial proteins including CaM that forms the core of this complex and mapped their locations in the RS complex (Table I).

The acidic nature of the majority of these proteins allowed the separation and characterization of RSP1-17 on Two-Dimensional (2D) gels (Piperno et al., 1977). They were identified based on their absence in the spokeless mutant (*pf14*) compared with that of Wild-Type (WT). By comparison of the RSPs in the 2D map of axonemes from mutants lacking entire or part of the RS, it was concluded that five subunits (RSP1, 4, 6, 9 and 10) are components of the spoke head while the others are present in the spoke stalk (Figure 1-4).

The extraction of radial spoke components from the axonemal microtubule using buffers containing 0.5-0.6 M Potassium Iodide (KI) allowed further characterization of this complex (Yang et al., 2001). While KI disrupts microtubule outer doublets, the extracted radial spokes remain as intact particles, which can be further separated by sucrose gradient sedimentation. The extracted spoke complex sediments as an intact 20S particle towards the bottom of a 5-20% sucrose gradient. This fraction contains the 17 RSPs as well as 5 co-sedimented proteins including CaM (Yang et al., 2001, 2006). Studies using the spokeless mutant (*pf14*), localization techniques and in vitro reconstitution suggest that RSP3 is located at the base of the spoke stalk (Johnson, 1995; Diener et al., 1993).

Name	Location in the Radial Spoke	Reference
RSP1	Head	Yang et al., 2006
RSP4		
RSP6		
RSP9		
RSP10		
	Neck	
RSP2		
RSP23		
RSP16	Stalk	
RSP3		
RSP11		
RSP7		
RSP12		
RSP5		
RSP20 (Calmodulin)		
RSP22 (LC8)		
RSP8		
RSP14		
RSP13		
RSP17		

Table I: List of all radial spoke proteins and their location in the radial spoke complex.

Proteins marked in bold are used as markers for spoke head, neck and stalk, respectively.

1.8 The Tri-Molecular Sub-Complex at the Head-Stalk Junction of RS Complex

Three stalk proteins are predicted to form a distinct sub-complex. In axonemes from the RSP2 mutant (*pf24*), RSP2, 23 and 16 are diminished and spoke head proteins are reduced (Huang et al., 1981; Patel-King et al., 2004; Yang et al., 2005) while the remaining stalk proteins are normal. Thus, RSP2, 23 and 16 are predicted to reside at the junction of the spoke stalk and spoke head referred to as the neck region (Figure 1-4).

RSP16 is a spoke-specific Heat Shock Protein 40 (HSP40). Unlike most of the RSPs, the spoke HSP40 does not join the precursors until their arrival in the flagellar compartment. RSP16 is not essential for the assembly of other RSPs. However, flagella lacking this protein display sporadic stalling (Yang et al., 2008). This study suggests that the addition of this evolutionarily conserved HSP40 towards the final stage of assembly enables RS to control sequential activation of dynein arms.

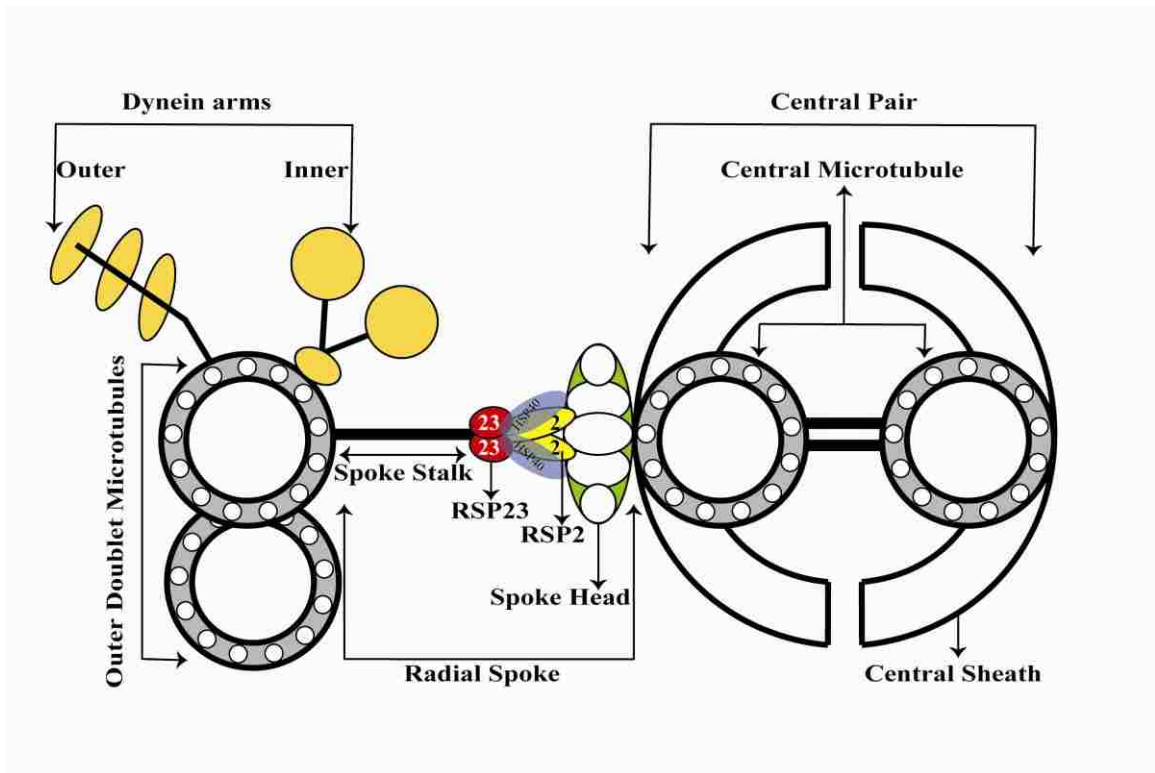


Figure 1-4: Schematic Showing RS-CP Interaction and Predicted Positions of RSP2, 23 and 16 (HSP40) in the Neck Region.

Transient interaction of the radial spoke with the central pair results in tilt and strain of the engaged radial spoke. This interaction controls the outer and inner dynein arms (ODA and IDA) which convert interdoublet sliding to flagellar bending and oscillatory beating. RSP2, RSP23 and RSP16 (HSP40) are proteins in the spoke neck predicted to interact with each other under the spoke head.

1.9 Goals of the Dissertation

This thesis focuses on RSP2 and 23 because of their intriguing features. Both proteins contain CaMB domains and share a poorly characterized DPY-30 domain. The DPY-30 domain is an evolutionarily conserved domain initially discovered as a member of the chromosome modification complex. It is similar in sequence and structure to the RIIa domain which is a dimerization and docking domain that anchors PKA to specific intracellular locations. DPY-30 domain is associated with different molecular domains in diverse proteins. Thus, it is not clear if this domain has a function similar to RIIa and why it is present in different types of proteins. Interestingly, only the N-terminus of RSP2 including the DPY-30 domain is conserved in higher organisms. In contrast, the CaMB motif of RSP2 is specific for *Chlamydomonas*. The other DPY-30 protein, RSP23, has a Nucleoside Diphosphate Kinase (NDK) domain and was discovered independently (Patel-King et al., 2004). NDK's are known to catalyze generation of triphosphates (like ATP or GTP). The putative human homolog of RSP23 (NDK-5) was found to be localized in the flagella of sperm (Munier et al., 2003). However, the role of an enzymatic domain in the RS is not clear. The goals of this study are to:

- 1) Elucidate the role of the evolutionarily conserved DPY-30 domain
- 2) Determine the importance of the CaMB motif of RSP2
- 3) Elucidate the significance of NDK activity of RSP23 in the RS

By generating mutants defective in these domains, this thesis has revealed the critical role of these proteins in the function and assembly of RS.

CHAPTER II: MATERIALS AND METHODS

2.1 Strains and Culture Conditions

C. reinhardtii WT strain (cc124) and previously defined RS mutants, *pf24* and *pf14* (Huang et al., 1981) were obtained from the *Chlamydomonas* Genetic Center (Duke University, NC). *pf14* lacks the entire RS due to the mutation of RSP3 gene (Luck et al. 1977). *pf24* has a reduced amount of spoke head and stalk due to defective RSP2 gene (Huang et al., 1981). Cells were grown in Tris-Acetate-Phosphate (TAP) medium in aerated photoheterotrophic conditions under a 14/10 hr light/dark cycle (Witman, 1986).

2.2 Sequence Analysis

BLAST search was used to identify putative homologs of RSPs. Sequence alignments of homologous proteins were generated using the ClustalW2 program (Larkin et al., 2007). The SMART (Simple Modular Architecture Research Tool) program (Schultz et al., 1998) was used to identify molecular domains in these proteins. COILS program (Lupas et al., 1991) was used to analyze propensity of regions to form coiled-coils. Homology modeling of RSP2 N-terminus was performed using the SWISS-MODEL 8.5 server (Arnold et al., 2006). PyMOL (DeLano, 2002) was used to improve the visualization of the model created.

2.3 Molecular Biology

2.3.1 Cloning

a) Generation of Bacterial Constructs

i) RSP2 Constructs

The full length RSP2 expression construct in pET28a (Yang et al., 2004) with a 6-His tag was used as WT control. CaMB* construct was created by mutating two Arg residues in the CaMB motif using PCR-based QuickChange Site-directed mutagenesis (Stratagene). The template was the RSP2 expression construct in pET28a (Yang et al., 2004). The complimentary primers are CalB5' and CalB3' in which R581 and R584 codons were replaced with those coding for glycine. These Arg residues were mutated to reduce the positive charge in the calmodulin binding amphipathic helix of the CaMB motif. For expression of MBP-RSP2₇₋₁₁₉ and MBP-RSP2₇₋₂₆₅, the coding sequence was amplified and cloned into pMCSG19 vector using a ligation-independent strategy by the Midwest Consortium for Structural Genomics (Argonne National Laboratory, Illinois) as described (Donnelly et al., 2006).

ii) RSP23 Constructs

The cDNA sequence of RSP23 (from a.a. 7-586) in the pMAL-c2 vector (King et al., 2004) was used as a template to generate RSP23 constructs. The codons for the N-terminal six amino acids were added to this construct using two consecutive PCR reactions. The first round of PCR used the sense primer NDKS with additional codons for a.a. 4-6 and KpnAS primers. The sense primer for the second round of PCR was

NdeS that includes the codons for first three a.a.. The NdeS-KpnAS PCR product (1101 bp) and KpnI-HindIII C-terminal fragment (660 bp) of RSP23 digested from the pMAL-c2 vector were ligated into pET28 vector which was digested with NdeI and HindIII to create the full length WT RSP23 construct. This plasmid did not produce detectable levels of recombinant RSP23. However, it was used as template to create His-tagged WT and mutant RSP23 constructs.

b) Generation of Constructs for Expression of RSP2 in *Chlamydomonas*

The genomic sequence of RSP2 was released from an RSP2 genomic subclone in pBluescript vector (Yang et al., 2004) by NcoI digestion and cloned into the pGEM-T Easy vector. This plasmid was used as a template to generate mutant constructs. The sequences of primers used for generation of all constructs are listed in Table I.

i) Δ DPY-30

The nucleotide sequences upstream and downstream to the coding region of DPY-30 domain was amplified from the WT construct using the following primer pairs named after the convenient restriction sites in the gene:

(i) Bam (BamHI) and H' (HindIII) (ii) H'' (HindIII) and Nru (NruI)

The PCR products of Bam- H' (1000 bp) and H''-Nru (150 bp) replaced the BamHI-NruI fragment of WT RSP2 plasmid, leading to a 32 a.a. deletion in the DPY-30 domain (Fig. 2-1).

ii) Δ CT-Tag

To create a tagged construct, the p3HA plasmid (Silflow et al., 2001) was converted into p3HA-6His using PCR and primers containing His codons. To create the

Δ CT-Tag construct, the tag sequence was amplified using p3HA-6His plasmid as a template and a primer pair, XhoS_{HA} and XhoAS_{HA} with a built-in Xba site and stop codon. The 150-bp PCR product was cloned into XhoI site preceding the coding sequence for the C-terminal 16 a.a. in WT RSP2 gene. This cloning strategy resulted in the addition of a 3HA-6His tag and deletion of the C-terminal 16 a.a. of RSP2 (Fig. 2-1). The additional Xba site in the antisense primer was used for creating RSP2₁₋₁₂₀ construct.

iii) Δ CT

The Δ CT construct was created by amplifying the WT construct with primers BsrG and Xho which included a stop codon. The PCR product (440 bp) with a stop codon replaced the original sequence in the WT plasmid.

iv) RSP2₁₋₁₂₀

The N-terminus of RSP2 gene was PCR-amplified using primers, Bam and EcoRIAS. The sequence coding for 3HA-6His tag was amplified using EcoRIS_{HA} and XbaAS_{HA} primers. The PCR products of Bam-EcoRIAS (1600 bp) and EcoRIS_{HA}-XbaAS_{HA} (150 bp) were cloned between BamHI site and XbaI site of the Δ CT-Tag plasmid (Fig. 2-1).

v) CaMB*

The 440 bp region containing the mutated CaMB sequence in CaMB* cDNA construct was released by BsrGI and XhoI restriction digest and cloned into the respective sites in the WT plasmid (Fig. 2-1).

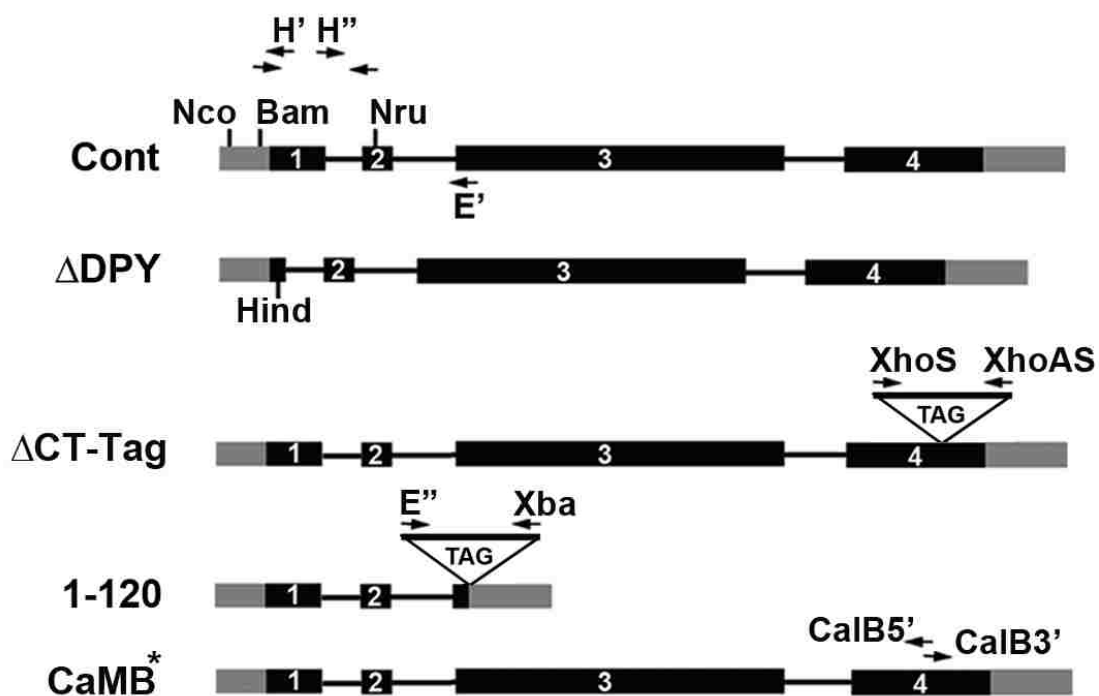


Figure 2-1. Creation of RSP2 Deletion and Mutation Constructs.

ΔDPY construct was generated using 2 sets of primers (Bam-H' and H''-Nru) to delete 32 a. a. of DPY-30 domain. Primer pairs, Bam-E', E''-Xba and XhoS-XhoAS, were used to create the two tagged C-terminal deletion constructs, 1-120 and ΔCT-Tag. CaMB* was created using CalB5' and CalB3' primers.

c) Generation of Constructs for the Expression of RSP23 in *Chlamydomonas*

To generate RSP23 expression constructs for *Chlamydomonas*, RSP23 cDNA was cloned into a vector, pPMM-LC8-6His plasmid which contains a Paromomycin (PMM)-selection cassette and the 6His-tagged LC8 gene. Primers NDKBglS and NDKBglAS were used to amplify the RSP23 cDNA and to add BglII restriction site for cloning. The vector including the LC8 flanking sequence and the His tag were amplified using a primer pair LC8BglS and LC8BglAS (Yang et al., 2009). The two PCR products were band purified and ligated together, designated as NDKWT. Using NDKWT as template, site-directed mutagenesis was performed using NDKH2AS and NDKH2AAS primers to mutate the Histidine residue (H121) in NDK to alanine. This plasmid was designated as NDKMut.

2.3.2 Generation of RS Mutant Strains

Electroporation (Shimogawara et al., 1998) was performed to introduce deletion constructs into the RSP2 mutant, *pf24*. The RSP2 constructs were expressed along with a selection plasmid, pSI 103, which confers PMM resistance. Briefly, autolysin-treated cells were washed with TAP medium containing 40 mM sucrose and resuspended in the same solution to a final concentration of 1×10^8 cells/ml. A 125- μ l aliquot was placed in a 2-mm electroporation cuvette (model 620; BTX Technologies, Inc.) and subjected to an electric pulse (ECM 630 electroporation apparatus; BTX Technologies, Inc.) of 360 V for 2 milliseconds (500 V/capacitance and resistance, 25 μ F capacitance and 125 Ohms). The cells were allowed to recover for 60 mins under light after addition of 10 ml TAP-sucrose solution. After 1 hr, the cells were centrifuged gently and washed three

times with TAP medium. Finally, the cells were resuspended in TAP medium and allowed to recover overnight. After 24 hours, the cell suspensions were plated on TAP agar plates with 10 µg/ml PMM.

RSP23 constructs were transformed using the glass bead method as described previously (Yang et al., 2006) with minor modifications. The WT cc124 cells were treated with autolysin at 1×10^7 cells/ml for 1 hr until >50% cells were lysed by 0.5% NP-40 treatment. Cells were gently spun down and resuspended in TAP medium at 1×10^8 cell/ml (Harris, 1988). The plasmid at a concentration of 2.0, 4.0, 6.0 or 8.0 µg, 300 mg of glass beads, and 100 µl of freshly prepared 20% PEG 8000 were added to 5 ml cells, and the mixture was vortexed at speed 8 (Mini-Vortexer; VWR, West Chester, PA) for 45sec. The supernatant was decanted and immediately diluted with 10 ml of TAP medium. After centrifugation at 1500 X g for 5 min, cell pellets were resuspended in 5 ml TAP medium, shaken gently under bright light. Following 24 hr recovery, cell pellets were resuspended and plated on 12 µg/ml PMM//TAP plates. The concentration of antibiotic was higher than 10 µg/ml PMM used for RSP2 mutant *pf24* because of higher resistance.

2.4 Screening of Transformants

2.4.1 96- well Method for RSP2 transformants

Single colonies that formed 4–5 days after transformation were re-streaked on TAP plates. After 5 days under bright light, the transformants were resuspended in TAP medium in 96-well plates and screened for motility using inverted and upright compound microscopes (Olympus IX51 and BH-2).

2.4.2 Flagella Prep for RSP23 Transformants

Single colonies that formed 4-5 days after transformation were transferred to fresh TAP plates. After 5-6 days, cells were recovered and flagella were prepared for western blot analyses. Briefly, cells were scraped from the 5-6 day old plates and resuspended in 5 ml water containing 5.44 mM CaCl₂. The suspension was placed under light for 1 hr to stimulate flagella generation. Subsequently, cells were collected by centrifugation for 10 min at 1500 X g (Sorvall RC 6+, Thermo Scientific). The pellet was resuspended in 5ml of HMDS (10 mM Hepes, 5 mM MgSO₄, 1 mM Dithiothreitol and 4% Sucrose) solution and deflagellated with 0.013 mM dibucaine. The flagella-containing supernatant was collected after centrifugation at 1500 X g for 10 min. A 25% sucrose cushion in HMDS was then added to the supernatant which was then centrifuged at 1500 X g for 10 min. The supernatant was subjected to centrifugation at 13,000 X g for 5 min and the flagella-containing pellet was resuspended in buffer A (10 mM Hepes, 5 mM MgSO₄, 1 mM Dithiothreitol, 0.5 mM EDTA, 30 mM NaCl, 0.1 mM PMSF, 0.5 TIU/ml Aprotinin, pH 7.4) and fixed with 5X electrophoresis sample buffer and analyzed by Western blot.

2.5 Biochemistry

2.5.1 Axoneme Preparation

Axonemes were prepared as described previously (Yang et al., 2008). Briefly, *Chlamydomonas* cells were harvested and deflagellated using the dibucaine method (Witman, 1986). Flagella were demembrated with 0.5% Nonidet P-40 (Calbiochem)

in buffer A, and axonemes were washed once with buffer A. Axonemes were sedimented by centrifugation and resuspended in buffer A. Protein concentration was determined using the Bradford assay (BioRad) using Bovine Serum Albumin (BSA) as standard.

2.5.2 Isolation of RS Complex by Sucrose Gradient Fractionation

To extract RS, axonemes were resuspended in 0.5 M KI in buffer A (5 mg/ml protein, 30 min on ice), followed by centrifugation at 12,000 X g for 10 min. The supernatant was dialyzed in buffer A for 1 h at 4°C and then clarified by centrifugation. An aliquot of 0.7 ml supernatant was loaded on an 11.5 ml 5–25% sucrose gradient made in buffer A and sedimented at 35,000 X g (SW41 rotor; Beckman Coulter) at 4°C for 16 hrs. Subsequently, fractions were collected. Sedimentation coefficients were estimated as described before (Mitchell and Sale, 1999) using dynein and central pair apparatus complexes as standards. For SDS-PAGE, aliquots of the fractions were mixed with 5 X electrophoresis sample buffer. Pellets and supernatant were processed for Western blot analysis.

2.5.3 CaM Affinity Purification

CaM affinity purification experiments were performed as described (Yang et al., 2004) with minor modifications. All four RSP2 expression constructs were transformed into BL21 (DE3) cells. Antibiotic-resistant single colonies were grown in LB medium to an OD of 0.4-0.6. Protein expression was induced by addition of 0.1 mg/ml IPTG and

incubation at 16°C for 16 hrs. The bacterial pellet was resuspended in CaMB buffer (60 mM NaCl, 50 mM Tris, pH 7.5) and sonicated using 10 second pulses on a Branson Digital Sonifier. The mixture was centrifuged at 11,500 X g for 30 min and the supernatant was supplemented with Aprotinin, Phenylmethylsulfonyl fluoride, complete protease inhibitor cocktail (Roche, Indianapolis, Ind.), and 2 mM CaCl₂. Following overnight incubation with CaM-agarose beads (Sigma) and washing with CaMB buffer containing 2 mM Ca²⁺. Elution was carried out with 2 mM EGTA in the CaMB buffer.

2.5.4 SDS-PAGE

Different percentages of acrylamide and bis-acrylamide SDS-PAGE gels were used, as indicated. Protein samples were fixed with 5X sample buffer and boiled at 100°C for 5 min. The fixed samples and molecular weight marker (Fermentas) were loaded into the gel.

2.5.5 Protein Gel Transfer

For western blot, proteins in SDS-PAGE gels were transferred onto nitrocellulose membranes (with a 0.2 µm pore size for proteins smaller than 40 k Da and 0.45 µm for larger proteins) at 100 V for 45 or 60 min depending on the protein size. The proteins were visualized by staining Ponceau S solution (0.2% Ponceau S, 3% Trichloroacetic acid) for 5 min and destaining with double distilled water.

2.5.6 Western Blot Analysis

After electro-transferring, the blot was incubated with 5% non-fat dry milk (Blotto) prepared in 1X TBS (547 mM NaCl, 10.7 mM KCl, 99 mM TrisBase, pH 7.5) for 1 hr at room temperature. Subsequently, the blot was incubated with appropriate primary antibody (1:5000) in Blotto for 1.5 hr at room temperature (or as indicated). After washing with 1X TBS three times, 5 min each, the membrane was incubated with appropriate Horse Radish Peroxidase (HRP)-conjugated secondary antibody in Blotto for 1.5 hr at room temperature. After washing with TBS, the blot was subjected to Enhanced ChemiLuminescence (ECL) using a mixture of equal volumes of solution 1 (500 μ l 1M Tris-Cl pH 8.8, 4.4 ml H₂O, 22 μ l Coumaric acid (15 mg/ml in DMSO), 50 μ l luminol (44 mg/ml in DMSO) and solution 2 (500 μ l 1M Tris-Cl pH 8.8, 4.5 ml H₂O, 3 μ l H₂O₂). The membrane was immersed in this solution for 1 min and exposed to X-ray film. The film were developed using an automated film processor Cp 1000 (AGFA). List of primary antibodies used against RSPs and tags are listed in Table II.

2.5.7 Western Blot for CaM

Western blots using anti-CaM antibodies were carried out as described (Wargo et al., 2005). Proteins separated on a 14% acrylamide gel were transferred to a PVDF membrane (Immobilon-P, Millipore) for 30 mins at room temperature. The membrane was rinsed quickly in TBS and then fixed in TBS with 0.2% glutaraldehyde for 30 minutes. Following a 5min rinse, the blot was blocked for 1 hr in TBS with 5% BSA/TBS (Sigma-Aldrich, St Louis, MO, regular fraction V, A-7906) at room temperature. After a brief rinse in TBS, blots were incubated with anti-CaM antibody (1:7000) in 1%

BSA/TBS at 37°C for 2 hrs. After washes with 0.05% Tween-20/TBS, the membrane was incubated with anti-rabbit secondary antibody in 1% BSA/0.05% Tween-20/TBS (37°C for 1.5 hrs). Following, final washes with 0.05% Tween-20/TBS, the antibody reactivity was revealed by ECL.

2.6 Motility Analyses

The motility analyses were performed as described previously (Yang et al., 2008). Microscopy was performed at 200-400X magnification using bright field compound microscope (Nikon). For low speed video microscopy, control and mutant cells were digitally recorded using a Charge-Coupled Device CCD camera (CoolSNAP ES; Photometrics) at a maximum rate of 20 frames/sec. MetaMorph imaging system (version 6.1r5, Molecular Devices, Sunnyvale, CA) was used to track the movement of individual cells and calculation of swimming velocities (Yang and Yang, 2006). For high speed video microscopy, MotionPro HP-3 camera (Redlake) was used at a rate of 500 frames/sec. Gooseneck lamp with two fiberoptic guides and tungsten light source (Model DL-150, Fryer Company, IL) was used for altering the directions of illumination and to replace the light source from the microscope.

For testing the dependence of calcium, cells were resuspended in solutions as indicated and observed immediately and every 5 mins under dim and normal light settings. The light intensity (in lux) was measured using a light meter (Model #840010, Sper Scientific, AZ).

Table II Sequences of Primers Used

Name	Sequence (5'-3')
Bam	cttctacacggatccgccggtctcc
Hind H'	cgaagctttgggtcggagccattcttgagtgc
Hind H''	agaagcttctgggcctatggctgctcaagtaagc
Nru	caaatcctgttgccgctcgcga
EcoRIAS	tgggaattcggctgtgtgctgcttgaccag
EcoRIS_{HA}	tcggaattcagcagccggggaggcctgtcg
XbaAS_{HA}	tgctctagagcttagtggtgggtgggtgctc
CalB5'	catcaagcaggtgcgggaggtggcggacaaggcagt
CalB3'	gcagcactgccttgcgccacctcccgcacctgct
XhoS_{HA}	actcgagcagccggggaggcctgtcgcga
XhoAS_{HA}	tctcgagtctagatcagtggtgggtgggtgg
BsrG	gacgcggagatgccgaacacgctg
Xho	gctgctcgagcttagtgcacctcctgggccggctg
NDKS	gctagaaaagacttccgcgtaataagccagatgc
KpnAS	g'gcacatcaccgccacctcctccg
NdeS	tccatatggcagagctagaaaagactttcg
NDKBglS	taagatctcatatggcagagctagaaaagactttcgcg
NDKBglAS	aaagatctctcagcggcctccggctccggctc
LC8BglS	gcagatctggcggccaccaccaccaccactaag
LC8BglAS	cgagatctcgccattttgctagtagttaggtgtggag

NDKH2AS	ggcaccagaatgccacc gcgggc agegactgcc
NDKH2AAS	gtaggcgagtcgctgcc gcgggt ggcattctgggtgcc

Table III Antibodies Used, their Host, Respective Antigens and Source Reference

	Antibody	Host	Antigen	Reference
Stalk base	RSP3	Rabbit	Purified axonemal protein	Diener et al., 1993
Spoke neck	RSP16	Rabbit	Recombinant protein	Yang et al., 2005
	RSP2	Rabbit	Purified axonemal protein	Yang et al., 2001
	RSP2 ₇₋₁₁₉	Rabbit	Recombinant protein	Unpublished
	RSP23	Rabbit	Recombinant protein	Patel-King et al., 2004
	RSP23 ₁₋₂₀₁	Rabbit	Recombinant protein	Unpublished
Spoke head	RSP1	Rabbit	Purified axonemal protein	Yang et al., 2006
	RSP4/6	Rabbit	Purified axonemal protein	Qin et al., 2004
	Anti-His polyclonal	Rabbit	6-His	Wang et al., 1999
	Anti-His monoclonal	Mouse	6-His	Prakash et al., 2004 Chuma et al., 2003
	Anti-HA	Rabbit	3HA	Covance

CHAPTER III: THE ROLE OF THE EVOLUTIONARILY CONSERVED N-TERMINUS OF RSP2

3.1 Introduction

The 9+2 axonemes are evolutionarily conserved in morphology as well as in fundamental mechanisms. Because of the structural complexity, studies on the motility machinery largely relied on *Chlamydomonas* that is amenable to a wide range of experimental approaches. Studies of motility mutants, flagellar proteome (Pazour et al., 2005) and comparative genomics (Li et al., 2004) revealed many orthologous genes from diverse organisms including humans. Those that are essential for motility are often conserved and this information has led to the discoveries of several causative genes for primary cilia dyskinesia (PCD).

However, the conservation of the *Chlamydomonas* radial spoke protein, RSP2, in full length, is not apparent despite the critical roles RSP2 plays in the assembly of the RS and thus motility. The RSP2 mutant, *pf24*, which contains a mutation in the translation initiation codon, is paralyzed and has diminished levels of full length RSP2 in the flagella (Huang et al., 1981; Yang, 2004). In addition, spoke head proteins (RSP1, 4, 6, 9 and 10) and spoke stalk proteins, RSP16 and RSP23, are also reduced in *pf24* (Huang et al., 1981; Patel-King et al., 2004; Yang et al., 2005). However, proteins located near the outer doublets appear normal. Thus it was proposed that RSP2, 16 and 23 are located underneath the spoke head for linking it to the spoke base which is anchored to the outer doublets.

BLAST search reveals that there are two RSP2 mammalian homologs (DYDC1 and DYDC2, DPY-30 Domain Containing 1 and 2). However, these short proteins were

only ~200 a.a. long and were similar to the N-terminus of RSP2. This chapter describes the experimental approach taken to test the hypothesis that these shorter molecules are orthologs of RSP2 and only this conserved N-terminus is essential for the motility. The results reveal the critical role of a poorly investigated domain and variations among 9+2 axonemes.

3.2 Results

3.2.1 Sequence Analyses of the Conserved RSP2 N-terminus

To elucidate the role of RSP2 N-terminus, the sequence was first analyzed using the program SMART (Schultz et al., 1998). Many newer molecular modules have been described since RSP2 was first discovered (Yang et al., 2004). Interestingly, the program predicted a DPY-30 domain in the N-terminus of RSP2 (a.a. 8-49) (Fig. 3-1A). This relatively newly discovered motif was named after the DPY-30 protein, a small but critical subunit of the chromosome modification complex responsible for X-chromosome dosage compensation in *C. elegans* (Hsu et al., 1995). DPY-30 proteins are also found to be subunits of the SET-1 like methyl transferase complex in many other eukaryotic organisms such as yeast, *Chlamydomonas*, *Drosophila* and humans (Nagy et al., 2002; Hsu et al., 1995; Lieb et al., 1996; Cho et al., 2007). Intriguingly, this domain is also present in the conserved N-terminus of another radial spoke protein, RSP23 that is predicted to co-assemble with RSP2. The importance of DPY-30 proteins and the presence of this domain in two co-assembled RSP's suggest that the DPY-30 domain in the conserved N-terminus is critical for the function of RS assembly.

The DPY-30 domain is homologous to RIIa domain which is the regulatory subunit of Protein Kinase A (PKA), known for Dimerizing and Docking (D/D) PKA to specific subcellular locations (Scott, 2006). These two ~ 40-a.a. domains are categorized as two families in the RIIa superfamily by the PFAM database (<http://pfam.sanger.ac.uk/family/DPY-30>). Each family in the clan includes nearly 200 molecules which are found under diverged molecular contexts while each organism expresses multiple proteins with either domain. For example, several human genes encode proteins with the RIIa domain (Table III). Some of them are isoforms of PKA regulatory subunits. However, the others do not contain any feature reminiscent of PKA suggesting that these RIIa family members have functions independent of cAMP and PKA.

Two RIIa domain proteins are subunits of the RS complex (Fig. 3-1B and Yang et al., 2006). RSP11 does not have additional distinguishing features but is required for flagellar motility in spent media (Yang et al., 2005) while RSP7 carries a string of putative EF-hands which are usually known to bind calcium.

Similarly, six human genes encode DPY-30 domain-containing proteins (Table IV). Three of them (NDK-5, ADK5 and ADK7) have motifs related to nucleotide metabolism such as NDK or adenylate kinase (ADK). In contrast, the other three molecules, the 99 a.a. DPY-30 protein, DYDC1 and DYDC2 (the putative RSP2 homolog) are rather small without any additional recognizable motif.

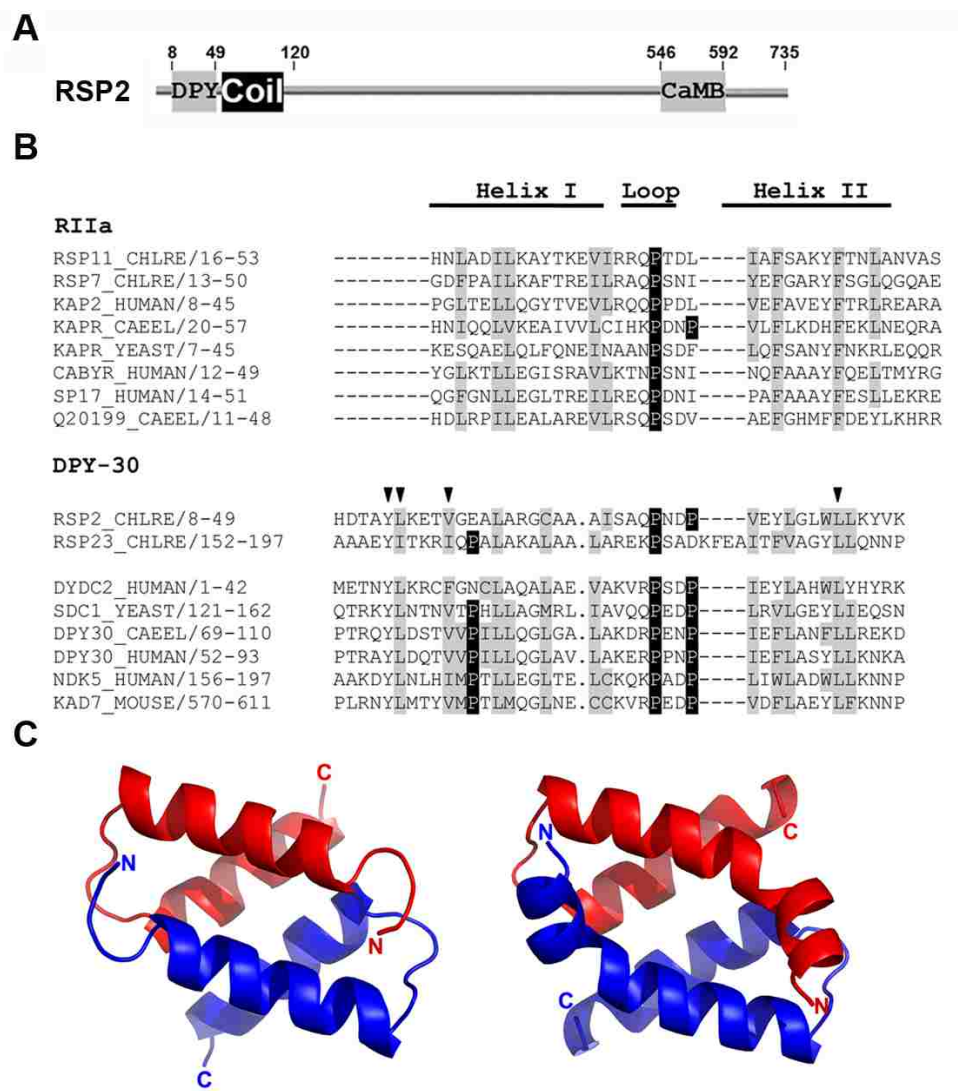






Figure 3-1. DPY-30 Domain in RSPs.

(A) Molecular domains in RSP2. (B) Sequence alignment shows the similarities between RIIa and DPY-30 domains in four *Chlamydomonas* RSPs and representative molecules from yeast and humans. The regions forming common helix-loop-helix structure are underlined. The conserved hydrophobic residues and prolines are highlighted in grey and black boxes. Helix I in DPY-30 domain with conserved residues (arrowhead) is longer. Accession Numbers for RIIa domain proteins: RSP11 (ABC02022) and RSP7 (ABC02026) are *Chlamydomonas* RSPs. KAP2 (NP_004148), CABYR (NP_036321) and SP17 (NP_059121) are human proteins; KAPR (NP_508999) and Q20199 are proteins from *C. elegans*. KAPR (NP_012231) is a yeast protein. Accession Numbers for RIIa domain proteins: RSP2 (XP_001702718.1) and RSP23 (XP_001698136) are *Chlamydomonas* RSPs; DYDC2 (NP_115748) , DPY30 (NP_115963) and NDK-5 (NP_003542) are human proteins; SDC1 (NP_010757) is a yeast protein; DPY30 (NP_506058) is a *C.elegans* protein and KAD7 (NP_689540) is a mouse protein. (C) Distinct conformations of RSP11 RIIa domain (left panel; a.a. #14-51) and RSP2 DPY-30 domain (right panel; a.a. # 9-50). The structures were modeled after the algorithms of mouse RIIa domain (PDB ID: 2IZY) and human DPY-30 domain (PDB ID: 3G36).

Sequence alignment of these putative D/D domains in the four RSPs (RSP2, 23, 11 and 7) and RIIa superfamily members shows that all of them contain conserved proline and hydrophobic residues in a helix-loop-helix module (Fig. 3-1B). However, helix I in DPY-30 domain is longer and forms a binding pocket distinct from that of PKA RIIa (Wang et al., 2009). Homology modeling using the crystal structures of respective domains from mammals (Wang et al., 2009; Gold et al., 2006) suggests that the RIIa domain of RSP11 and DPY-30 domain of RSP2 may have distinct binding surfaces (Fig. 3-1C). Based on the phenotypes of radial spoke mutants, these two types of similar domains probably dock to different parts of the RS complex.







In contrast to the 735-a.a. long RSP2, the closest mammalian homolog, DYDC2, consists of only ~200 a.a. (Fig. 3-2A). The homology around the N-terminus corresponding to the 40-a.a. DPY-30 domain is particularly high (Fig. 3-2B). Although the rest of the homologous region did not contain any recognizable motif, it has a propensity to form a coiled coil (Fig. 3-2C). Based on these analyses, it is postulated that only the conserved 120-a.a. region, including the DPY-30 domain and the coiled coil, is required for the assembly of a normal spoke head and thus oscillatory beating.

Protein	Acc. #	Gene ID	Domains	EST profile	Complexes/Function
KAP2 (404 a.a.)	NP_004148	5576		Broad	cAMP-dependent protein kinase alpha regulatory subunit
Ropporin (212 a.a.)	AAG27712	54763		Testis*	sperm flagella
CABYR (493 a.a.)	NP_036321	26256		Testis*, trachea*, pharynx*, ovary*, brain*, lung*, heart*, esophagus, muscle, uterus*	sperm flagella
SPA17 (151 a.a.)	NP_059121	53340		Testis*, parathyroid, prostate, uterus*, esophagus, ovary*, trachea*, bladder, adrenal gland, vascular, brain, eye, lung*	sperm surface protein 17

* Ciliated tissues

Table IV. RIIa Domain Containing Proteins in Humans.

KAP2 is a cAMP dependent protein kinase, Ropporin is Sperm Specific protein that binds rhophilin, CABYR is calcium-binding tyrosine phosphorylation-regulated protein and SPA17 is a Sperm Autoantigenic Protein. These four molecules represent the diverse forms of RIIa containing proteins found in humans. They differ significantly in length, associated functional moieties and expression profile. RIIa is not only associated with protein kinases (KAP2) but also found in non-PKA related molecules.

Protein	Acc. #	Gene ID	Domains	EST profile	Complexes/Function
DPY-30 (99 a.a.)	NP_115963	84661		Broad	Histone methyltransferase
ADK5 (562 a.a.)	NP_777283	26289		Broad	AMP+ATP ↔ 2 ADP
ADK7 (723 a.a.)	NP_689540	122481		Broad	AMP+ATP ↔ 2 ADP
NDK-5 (212 a.a.)	NP_003542	8382		Broad	NTP+NDP ↔ NDP+NTP
DYDC1 (177 a.a.)	NP_620167	143241		Testis* and brain*.	Unknown
DYDC2 (177 a.a.)	NP_115748	84332		Lung*, pharynx*, skin, testis*, ovary*, eye, placenta, brain and bone.	Unknown

* Ciliated tissues

Table V. DPY-30 Domain Containing Proteins in Humans.

DPY-30 is a subunit of the histone methyl transferase complex; ADK5 and ADK7 are adenylate kinases; NDK-5 is a Nucleoside Diphosphate Kinase; DYDC1 and DYDC2 are duplicated genes of which DYDC2 is highly similar to RSP2. These six molecules contain the DPY-30 domain but differ significantly in length, additional functional moieties and expression profile. **D**, DPY-30; **NDK**, nucleotide diphosphate kinase; **ADK**, adenylate kinase.

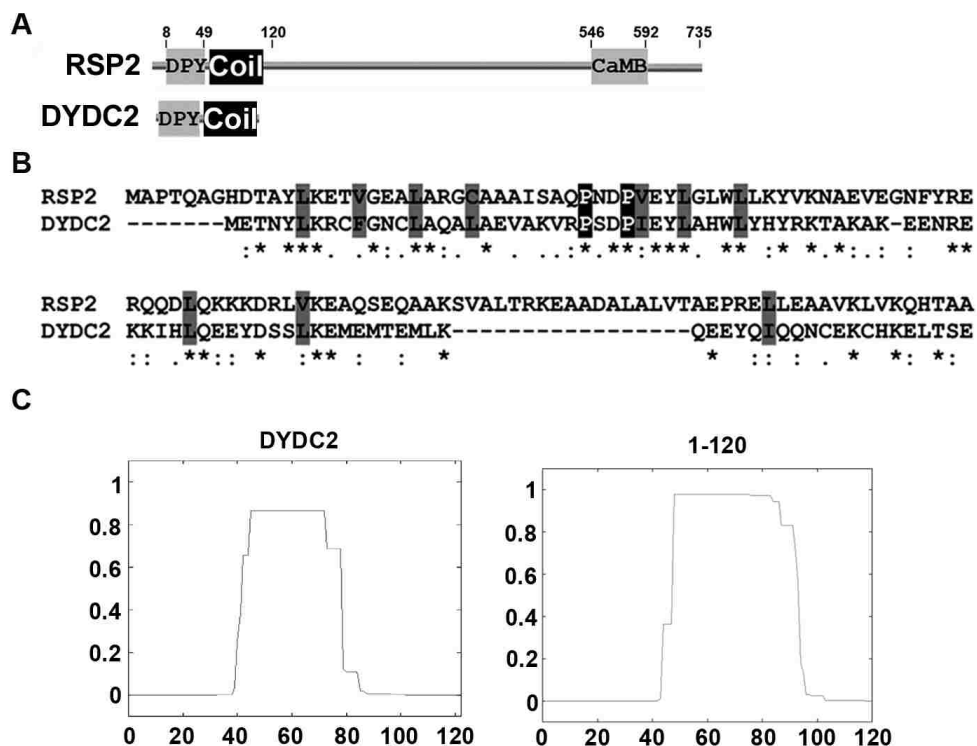


Figure 3-2. Comparison of the N-terminal 120 a.a. in *Chlamydomonas* RSP2 and Human DYDC2.

(A) Molecular motifs in RSP2 and its putative human homolog, DYDC2. Only the N-terminal moieties are conserved. The 1-8-14 (CaMB) is absent in DYDC2. (B) Sequence alignment of RSP2 and DYDC2 shows that the first ~40-a.a. regions corresponding to the DPY-30 domain are highly similar. The homology of the downstream regions is limited. Residues highlighted in grey represent hydrophobic residues (identical or similar but found in conserved positions among all DPY-30 family members); Proline residues highlighted in black form the loop region of the DPY-30 domain. * -identical residues, : -conserved substitutions and . -semi-conserved substitutions. (C) COILS program predicts a high propensity to form coiled coils in the downstream regions in both molecules.

3.2.2 DPY-30 Domain of RSP2 is Crucial for Flagellar Beating

To test the importance of DPY-30 domain, an RSP2 mutant lacking the DPY-30 domain was generated. Since targeted mutagenesis is not yet feasible in *Chlamydomonas*, the strategy is to express the deletion construct in the paralyzed RSP2 mutant, *pf24*. The rationale is that if the DPY-30 domain of RSP2 is crucial, the deletion construct will not rescue the paralysis of *pf24*. The RSP2 gene including the upstream and downstream flanking sequences was first cloned into pGEM-T Easy vector (Fig. 3-3). This plasmid was used as the control construct and as a template to generate the Δ DPY-30 construct. A PCR-cloning strategy was taken to create the Δ DPY-30 construct (as described in Chapter 2) that will express truncated RSP2 lacking the first 32 a.a. of the 41-a.a. DPY-30 domain. The last few a.a. in the predicted domain were retained to ensure the proper splicing of the first intron that disrupts the DPY-30 domain. The control and Δ DPY-30 constructs were transformed into *pf24* along with a selection plasmid, pSI103 that carries a PMM resistant gene (Sizova et al., 2001).

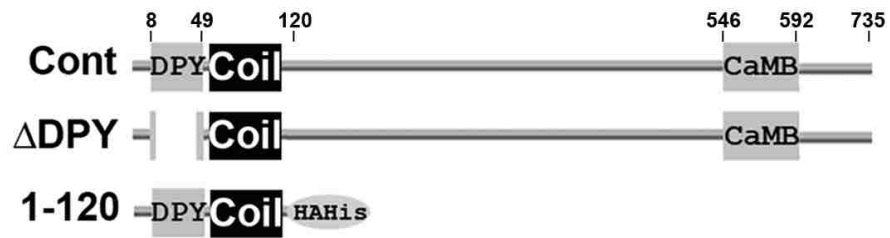


Figure 3-3. RSP2 Constructs.

Cont is the full length RSP2 used to rescue *pf24* mutant. Residues in RSP2 are labeled. Δ DPY RSP2 lacks 32 a. a. in DPY-30 domain. RSP2₁₋₁₂₀ contains the conserved DPY-30, the downstream coiled coil region and a 3HA-6His tag.

Approximately 100-200 antibiotic resistant clones were resuspended in 96-well plates and were screened using a bright field microscope. In the control group, 5.2% transformants swam like WT *Chlamydomonas*. These swimming clones along with some paralyzed clones were screened using a western blot to ensure the former expressed RSP2 and the latter did not. From this screening, strains expressing RSP2 at WT levels were selected for further assays. These transformants in which *pf24* is rescued with full length RSP2 served as Control (Cont) for all experiments. This method of screening and selection was used for isolating all control and mutant strains used in this study. In contrast to control, all Δ DPY-30 transformants were paralyzed. Upon further observation, it was found that approximately 10.4% of them were different from *pf24* and exhibited crossed flagella. Images of *pf24* and Δ DPY-30 transformants were recorded using low speed microscopy and a CCD camera. The paralyzed flagella of *pf24* cells were separated. By contrast, those of Δ DPY-30 cells tend to cross each other (Fig. 3-4).

Similar anomalies also occurred in the HSP40-minus flagella (Yang et al., 2008). The defect is due to stalled initiation of the power stroke. Normally, the power stroke starts prior to the completion of the of the preceding recovery stroke. Thus, the two flagella of WT *Chlamydomonas* rarely cross each other. When the initiation is delayed, the continued recovery stroke causes two flagella to cross each other and appear as a reverse bend (Yang et al., 2008).

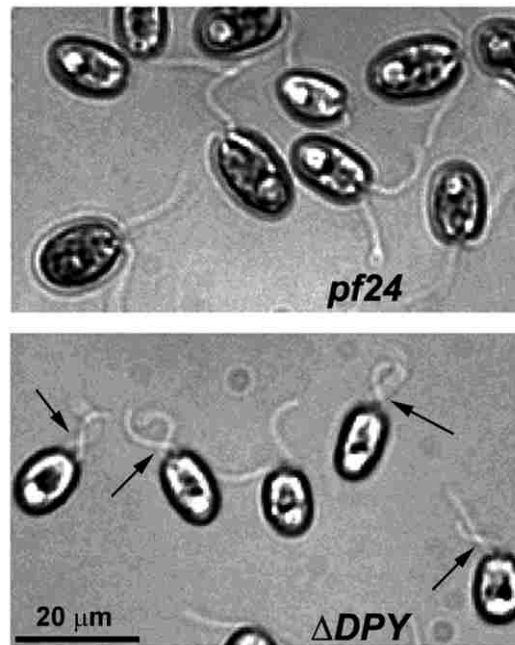


Figure 3-4. DPY-30 Domain of RSP2 is Crucial for Motility.

Cells lacking the DPY-30 domain (Δ DPY) are paralyzed. The flagella of mutants tend to appear crossed (black arrows, lower panel), unlike the widely separated flagella in *pf24* (upper panel) as shown by live cell imaging. Cells were recorded by Metamorph software.

3.2.3 The Conserved N-terminus of RSP2 is Sufficient for Motility

To test whether the conserved N-terminus is sufficient for the function of RSP2, the RSP2₁₋₁₂₀ construct was created using the control plasmid as a template (Fig. 3-3). Primers Bam and EcoRIAS were used to amplify the N-terminal 120 a.a. of RSP2 while primers EcoRIS_{HA} and XbaAS_{HA} amplified a 3HA-6His tag from the p3HA-6His plasmid (as described in Chapter 2). The RSP2₁₋₁₂₀ plasmid was expressed in *pf24* as described previously. 100-200 clones were resuspended in growth media and analyzed under a microscope. 4% of the RSP2₁₋₁₂₀ transformants were motile while the rest were paralyzed like the parental strain, *pf24*. These results suggest that the conserved N-terminal 120 a.a. of RSP2 can restore the motility. The detailed analysis of motility is described in Chapter 4.

3.2.4 RS Composition in RSP2 mutants

To assess the protein deficiencies in Δ DPY-30 and RSP2₁₋₁₂₀ strains, axonemes from transformants were prepared for western blot analyses (outlined in Chapter 2). The membrane was probed for the indicated RSPs to reveal the defects in the RS complex (Figure 3-5). The negative and positive controls were axonemes from the spoke-less mutant *pf14*, and from the control strain rescued with the full-length RSP2 construct (Cont). As expected for parental RSP2 mutant strain *pf24*, the spoke head proteins (represented by RSP1) and the spoke neck proteins (RSP23 and RSP16) were reduced drastically while the base of the spoke, represented by RSP3, appeared normal (Fig. 3-5). These defective proteins appeared normal in axonemes of the motile RSP2₁₋₁₂₀ strain and surprisingly, in the paralyzed Δ DPY-30 strain as well. These results suggest that the

conserved N-terminus of RSP2 is sufficient for restoring the biochemical deficiencies in *pf24* while the DPY-30 domain by itself is dispensable in the assembly of RS complex.

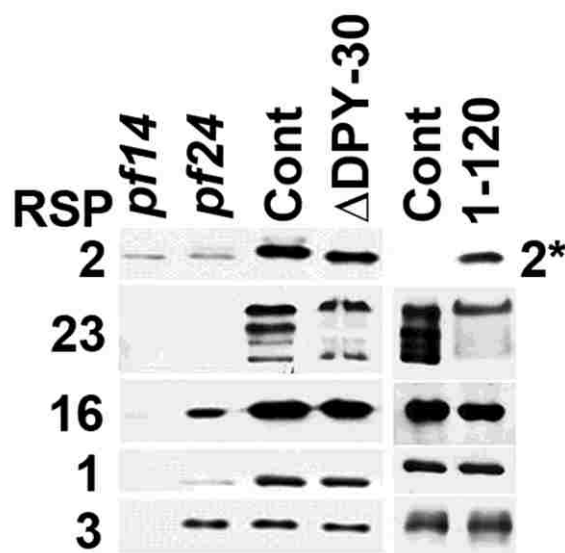


Figure 3-5. RSP2 Deletion Mutants Restore Biochemical Deficiencies of RS Complex.

Control (Cont) is *pf24* rescued with full length RSP2, Δ DPY-30 lacks the DPY-30 domain and RSP2₁₋₁₂₀ (1-120) has the conserved N-terminus of RSP2. Western blots of axonemes from spoke mutants and *pf24* transformants showed that the two truncated RSP2 polypeptides (Δ DPY-30 and 1-120) restore the RSPs deficient in *pf24*, represented by RSP1, RSP16 and the phosphoprotein RSP23. 2*, truncated RSP2 in 1-120 was decorated using HA antibody while the corresponding control doesn't have a band due to absence of a tag. The theoretical molecular weight of full length RSP2 is ~80 kDa while it migrates close to 110 kDa on a gel. Truncated RSP2 in the mutants migrates at 107 kDa (Δ DPY-30) and 15 kDa (1-120).

3.2.5 Stability of the RS Complex

To test if the paralysis of Δ DPY-30 is due to inappropriate assembly of RS, RS was extracted with 0.5 M KI buffer. The extracted spokes were further sedimented through a sucrose gradient. The fractions collected were analyzed by western blot using antibodies against representative RSPs. As anticipated for Control (*pf24* rescued with full length RSP2), all RSPs sedimented in a single peak as intact 20S particles (Fig. 3-6, top panel). In contrast, in the gradient of Δ DPY-30 mutant, truncated RSP2, RSP16 in the neck region and spoke head RSPs sedimented as distinct smaller particles (Fig. 3-6, compare arrows in top and middle panels) separate from the spoke base represented by RSP3. In the RSP2₁₋₁₂₀ mutant, RSP23 and RSP2₁₋₁₂₀, both containing DPY-30 domain, remained co-sedimented with RSP3 (Fig. 3-6, bottom panel). The spoke head proteins in the RSP2₁₋₁₂₀ mutant dissociated from the spoke base into separate particles. Thus, although all relevant RSPs are present in the RS complex in both mutants, RS assembly without the DPY-30 domain is flawed. The faulty assembly cannot support the oscillatory beating.

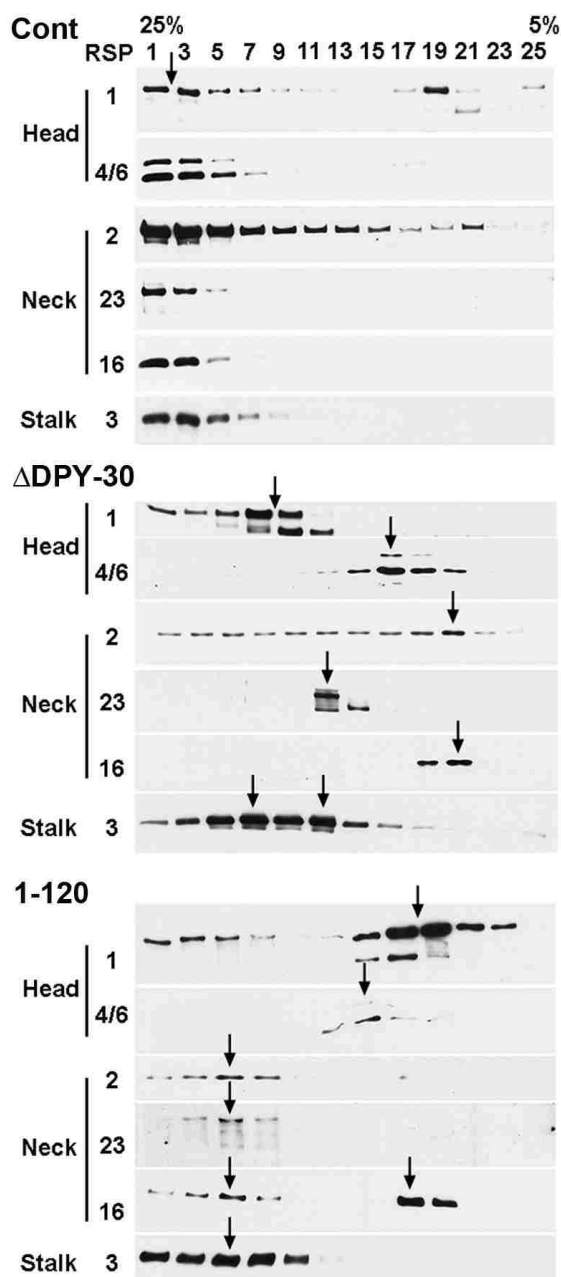


Figure 3-6. DPY-30 Domain is Required for the Stability of RS complex and Integrity of the Spoke Base.

The assembled RSPs in two RSP2 mutant strains dissociate differently. All RSPs in the control KI extract sediment as 20S particles in a 5-25% sucrose gradient (upper panel). In the Δ DPY-30 gradient (middle panel), the proteins in the spoke head, truncated RSP2 and RSP16 (HSP40) sediment in different peaks. In the RSP2₁₋₁₂₀ gradient (lower panel), RSP2₁₋₁₂₀ and RSP23 remain co-sedimented with RSP3 while only spokehead proteins dissociate. Arrows indicate the peak fraction of each protein.

3.3 Discussion

This chapter described the experimental approach taken towards elucidating the role of the RSP2 N-terminus.

3.3.1 The Conserved N-terminus of RSP2 is Sufficient to Restore Motility

The rescue of protein deficiencies and motility in the paralyzed RSP2 mutant with RSP2 N-terminal 120 a.a. indicates that this region links the spoke head and base modules. This finding is consistent with the sequence similarity of RSP2 with the shorter human proteins like DYDC2 and DYDC1 that are tandemly aligned on chromosome 10. Thus, these two genes of unknown function are likely to be orthologs of RSP2. This could be tested further by expressing the short human proteins in *pf24*. If the human proteins are orthologs of RSP2, they will restore swimming in *pf24*.

3.3.2 DPY-30 Domain of RSP2 is Crucial for Oscillatory Beating

The phenotype of the Δ DPY-30 mutant is rather intriguing. This truncated protein lacking 32 a.a of the 40-a.a. DPY-30 domain, rescues the biochemical deficiencies in *pf24* RS without rescuing the paralysis. It is possible that the paralysis is due to deletion-related misfolding. However, this explanation is inconsistent with the restoration of the missing RSPs. Thus, the simplest prediction is that the DPY-30 domain is critical for *Chlamydomonas* flagellar motility.

Although Δ DPY-30 mutants are paralyzed, the two paralyzed flagella cross each other, which is distinct from parental *pf24* strain or WT strain. The stalling of flagella at

crossed position suggests that the recovery stroke is not followed by the subsequent power stroke, leading to prolonged recovery stroke and crossed flagella.

This phenotype is similar to the flagella of mutants lacking RSP16, an RSP2-binding protein (Yang et al., 2008) or CP kinesin (Yokoyama et al., 2004). In the RSP16 mutant, flagella twitch actively but stall sporadically at different stages of the stroke. In contrast, Δ DPY-30 flagella rarely stall at the initiation of recovery stroke. The stalling suggests that the sequential activation of dyneins required for bend initiation and propagation is disrupted. This result strengthens the model that the RS functions to couple the mobile outer doublets and the CP. It is predicted that the RS is a rigid complex with slight elasticity. This physical property may be compromised when RSP16 or DPY-30 domain is absent. Interestingly, both RSP16 and DPY-30 are predicted to be dimers. The dimeric format is likely to be critical for the connection between the spoke head and base.

Since Δ DPY-30 can restore RS deficiencies in *pf24*, the dimeric DPY-30 domain must only be partially responsible for the assembly role of RSP2. Thus the sequence downstream to DPY-30, in particular, the coiled coil, may contribute to the assembly of the rigid junction.

3.3.3 KI-sensitivity of the Restored RS in the Two RSP2 Truncation Mutants

Despite the restoration of RS biochemical composition, the region around the spoke head in both truncated mutants is still abnormal. In contrast to the extraordinary stability of WT RS in 0.5 M KI, spokes in both mutants dissociated under similar conditions. However, the dissociation pattern of the two truncation strains differs. The

proteins retaining the DPY-30 domain remain co-sedimented with the spoke base while those lacking the DPY-30 domain dissociated into separate particles like the rest of spoke head. This suggests that the DPY-30 domain in RSP2 targets the spoke head region to the spoke base while the tethered sequence associates with the spoke head components. One of the proteins in the stalk base must anchor the DPY-30 domain. In this sense, DPY-30 may play a similar role as RIIa, albeit the tethered function is for the assembly of a structural complex.

CHAPTER IV: THE ROLE OF THE CALMODULIN-BINDING C-TERMINUS OF RSP2

4.1 Introduction

Calcium is a universal signaling molecule for motile cilia and flagella. As calcium in the cytoplasm is ~1000-fold lower than the extracellular concentration, increases in calcium concentration can trigger a range of motility changes, like flagellar dominance, phototaxis, increased beat frequency, quiescence and backward swimming (reviewed in Smith and Yang, 2004). Interestingly, several studies have shown that many calcium-binding proteins or calcium sensors are present in the axoneme (Yang et al., 2001; Wargo et al., 2005; Dymek et al., 2007). The number far exceeds known calcium-induced responses (Pazour et al., 2005). This suggests that calcium-mediated responses are more elaborate than recognized.

Calmodulin (CaM), the prototype calcium-sensor, is present in various cilia and flagella. In fact, CaM is much more abundant than most of the flagellar proteins. It is found in the detergent soluble fractions as well as in the axoneme. Studies using CaM-inhibitors suggest that this small molecule regulates flagellar movement. However, these inhibitors are of low specificity and are selective for cilia and flagella in certain organisms. CaM binding proteins can be investigated to elucidate the role of CaM in flagellar motility.

RSP2 and RSP23, which are predicted to co-localize near the spoke head, are the first Calmodulin-Binding (CaMB) proteins in flagella that have ever been discovered in axonemes. Sequence analysis predicted that the CaMB sites are located in the two basic amphipathic helices around a.a. 546-559 and 579 -592 near the C-terminus of RSP2

(Yang et al., 2004). Sequences in these two regions matched the “1-8-14” Ca²⁺-dependent CaMB motifs (Fig. 4-1A). CaM-affinity purification experiments using recombinant full length RSP2 revealed that this protein bound CaM in a calcium-dependent manner (Yang et al., 2004).

Intriguingly, BLAST search shows that the C-terminus of RSP2 is not conserved in higher organisms except in newly sequenced flagellate algae (*Micromonas pusilla*) and moss (*Psychomitrella sp.*) that are closely related to *Chlamydomonas*. This suggests that the C-terminus in RSP2 is conserved to facilitate behaviors specific to these simple organisms. RSP2 mutants were created to test this hypothesis. Although the RSP2 strain lacking the C-terminal CaMB region (1-120) is motile, their motility under a microscope is abnormal. Studies of these C-terminal mutants reveal a new role for this region and CaM.

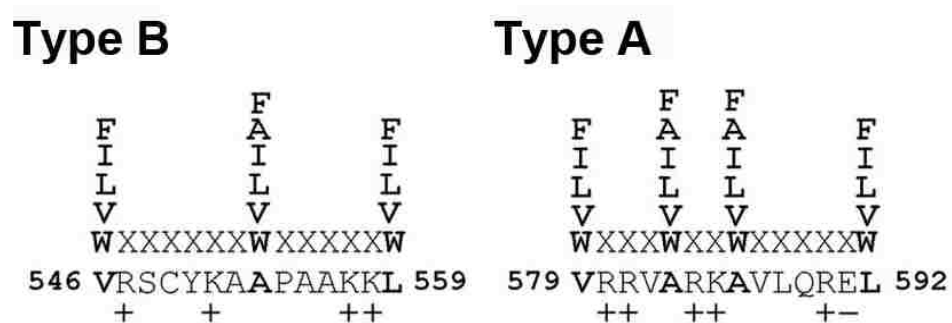


Figure 4-1. Calmodulin-Binding Sites in RSP2.

The basic amphipathic helices in the CaMB region contain the conserved hydrophobic residues (boldface) and multiple basic residues characteristic of type A (residues 579 to 592) and type B (residues 546 to 559) 1-8-14 calcium-dependent CaMB motifs. 1-8-14 refers to the position of hydrophobic residues in the amphipathic helix.

4.2 Results

4.2.1 C-terminus of RSP2 Maintains Helical Trajectory of Cells in Bright Light

RSP2₁₋₁₂₀ cells appear agitated under the microscope. However, their movement was indistinguishable from control when the light intensity was reduced. To further define the phenotype, cells were recorded at different light intensities and analyzed using Metamorph imaging software. At illumination below 1 klux (Dim, D ~60 lux in Figure 4-2, as measured on top of the slide) or under a red filter (25A), RSP2₁₋₁₂₀ cells swam with a fairly helical path like control cells. However, when the light is increased (Normal, N ~1 klux in Figure 4-2) or when the filter is removed, the helical trajectories become irregular (Figure 4-2, right panel).

The irregular movement was found to be reversible (Figure 4-3). Cells under the microscope were subjected to Dim (D), Normal (N) and Dim (D) light consecutively. Once the intensity was shifted to 1 klux (N), RSP2₁₋₁₂₀ cells lost their helical trajectories. However, they quickly regained swimming trajectory when light was shifted to dim. These results suggest that the C-terminus is involved in maintaining proper helical swimming under higher illumination.

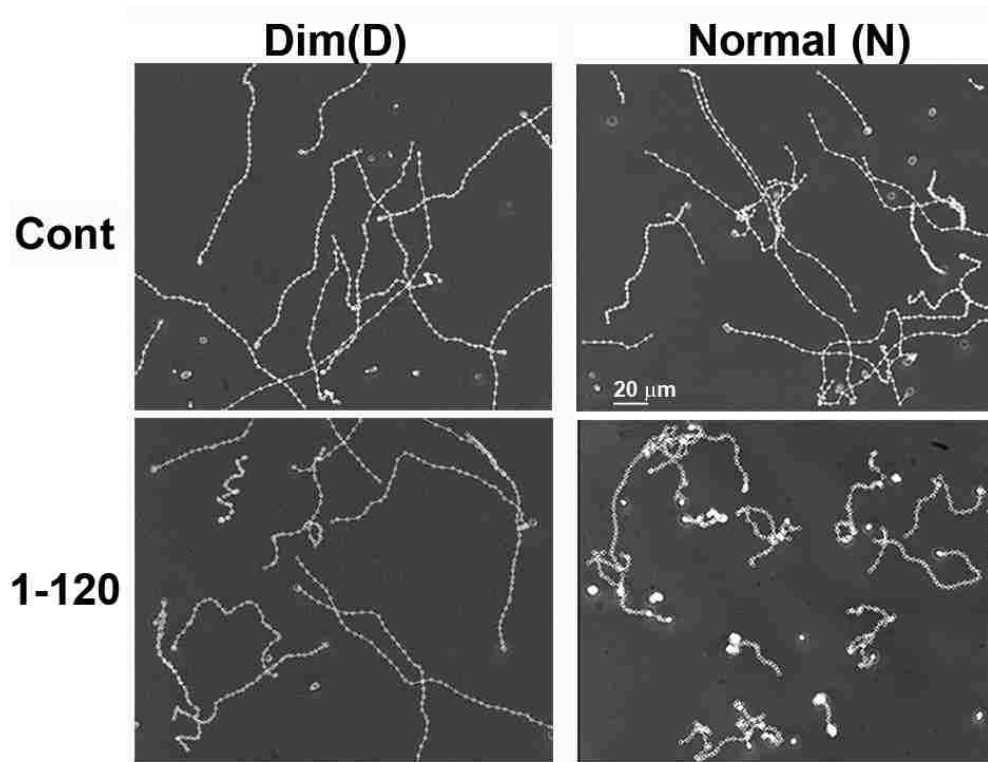


Figure 4-2. Mutant Lacking C-terminus of RSP2 Displayed Irregular Swimming Path Under Increased Light Intensities.

Control (Cont) and 1-120 cells were exposed to Dim light (D) of ~60 lux. Cell movement was recorded and tracked using Metamorph software. The intensity of light was increased to Normal (N) of about 1 klux and the motility was recorded. The tracked movements showed that 1-120 cells swam like control under dim light. However, under normal illumination mutant cells displayed irregular trajectories when compared to control.

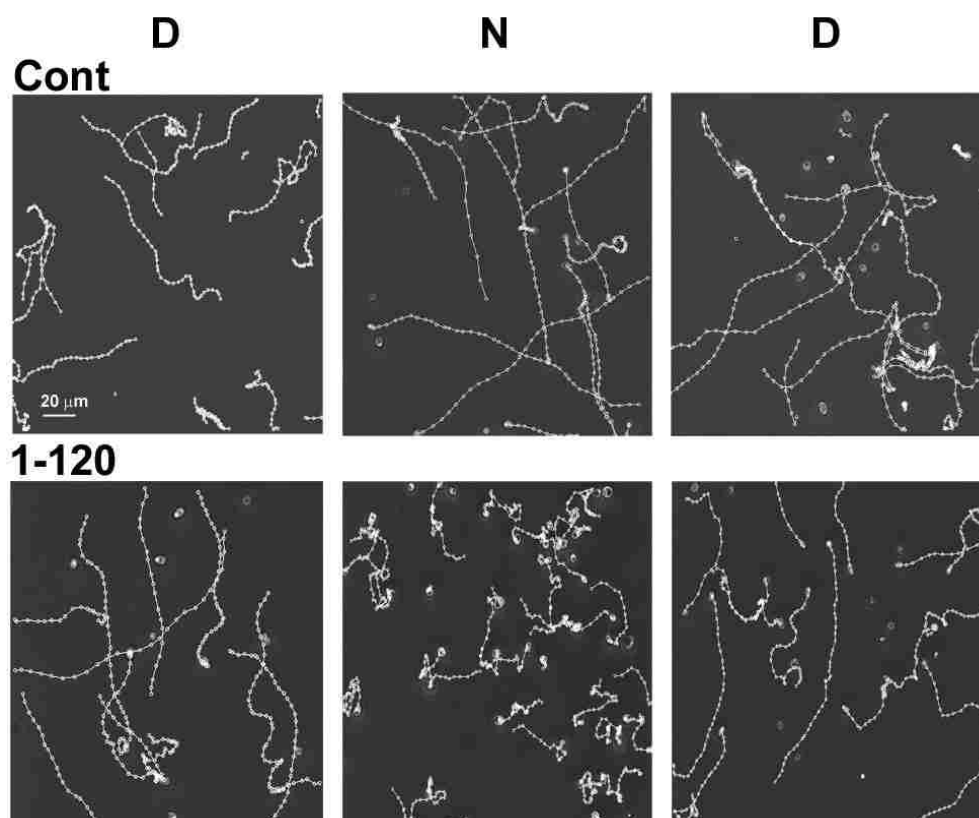


Figure 4-3. Irregular Trajectory of Mutant Cells was Reversible and Dependent on Illumination Levels.

Control and 1-120 cells were exposed to Dim, Normal and Dim light intensities while recording continuously. The intensities (lux) are the same as Figure 4-2. 1-120 cells moved with irregular trajectories when light intensity shifted from dim (D, 60 lux) to normal (N, 1 klux). The anomaly disappeared when the intensity was reduced. The movement of WT control (cont) under identical conditions did not change significantly.

4.2.2 Irregular Trajectory of Mutants is not Due to Impaired Photoaccumulation

To test if the unusual light-induced movement of $RSP2_{1-120}$ mutant cells was due to defective phototaxis, $RSP2_{1-120}$ strains were assessed using a photoaccumulation assay in which the movement of cells exposed to light is observed (Okita et al., 2005). Control and 1-120 cells in a Petri dish were exposed to a dual fiberoptic-guided gooseneck tungsten lamp with direction of light parallel to the bottom of the dish (Figure 4-4, arrows). Both strains accumulated in a similar manner towards light at 4 klux (Figure 4-4) or at ambient light, typical of positive phototaxis. The light response was reversible and similar for Control and $RSP2_{1-120}$ mutant cells at various light intensities. Both strains also displayed similar phototaxis and photoshock responses using stringent methods described previously (Moss et al., 1995). These results suggest that $RSP2_{1-120}$ cells have normal phototaxis and photoshock response.

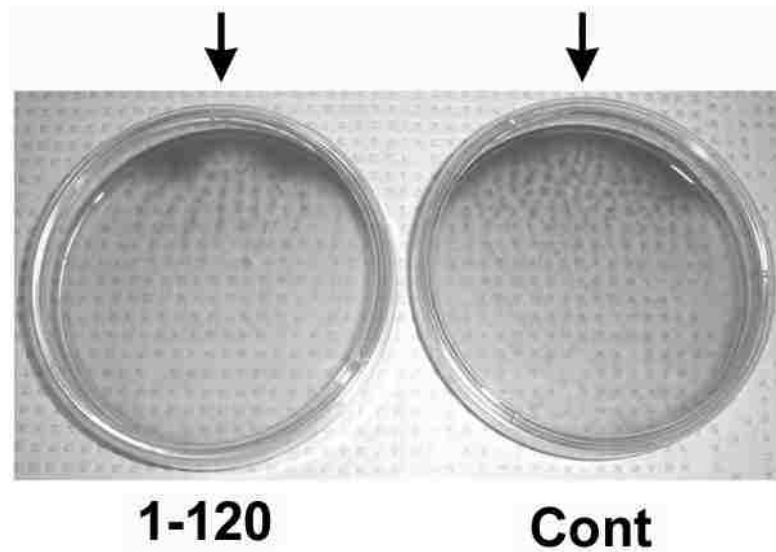


Figure 4-4. RSP2₁₋₁₂₀ and Control Cells Photoaccumulate in a Similar Manner.

RSP2₁₋₁₂₀ strain (1-120) and Control strain (Cont) are equally phototactic in photoaccumulation assay. Cells suspended in a Petri dish were exposed to light (4 klux) with an orientation parallel to the dish bottom (arrows). At this intensity, both strains displayed positive phototaxis.

4.2.3 Irregular Trajectory of RSP2₁₋₁₂₀ Cells is Dependent on Direction of Illumination

Although RSP2₁₋₁₂₀ strains displayed irregular movement under a microscope (at a light intensity of ~ 1 klux), their photoaccumulation pattern to much more intense illumination (~20 klux) in a Petri dish was indistinguishable from the control. Thus light intensity alone cannot account for the anomaly of the mutants. One difference in these two experiments was the orientation of light. Under a bright field microscope, the glass slide or cover slip obstructs the path of cells swimming towards or away from the illumination. If the glass barrier contributed to the anomalies, changing the direction of incident light in a microscope will reduce or abolish the irregular trajectory of RSP2₁₋₁₂₀ cells. To test this, the tungsten light bulb of the microscope was replaced with the tungsten lamp of a gooseneck fiberoptic that allows altering light directions. Using this setup, the light beam was oriented parallel to the glass slide (Figure 4-5, schematic) in an orientation similar to that used in the photoaccumulation assay. The trajectories of mutant and control cells were similar (upper panels) even at 6 klux intensity. However, mutants immediately displayed irregular movement when the illumination was turned vertical, similar to the direction of a microscope light source (Figure 4-5, right panel). Under this condition, WT trajectories also appeared slightly irregular but less pronounced than mutants (Fig. 4-5, left panel). This effect may be due to the unfocused light from the gooseneck fiberoptic.

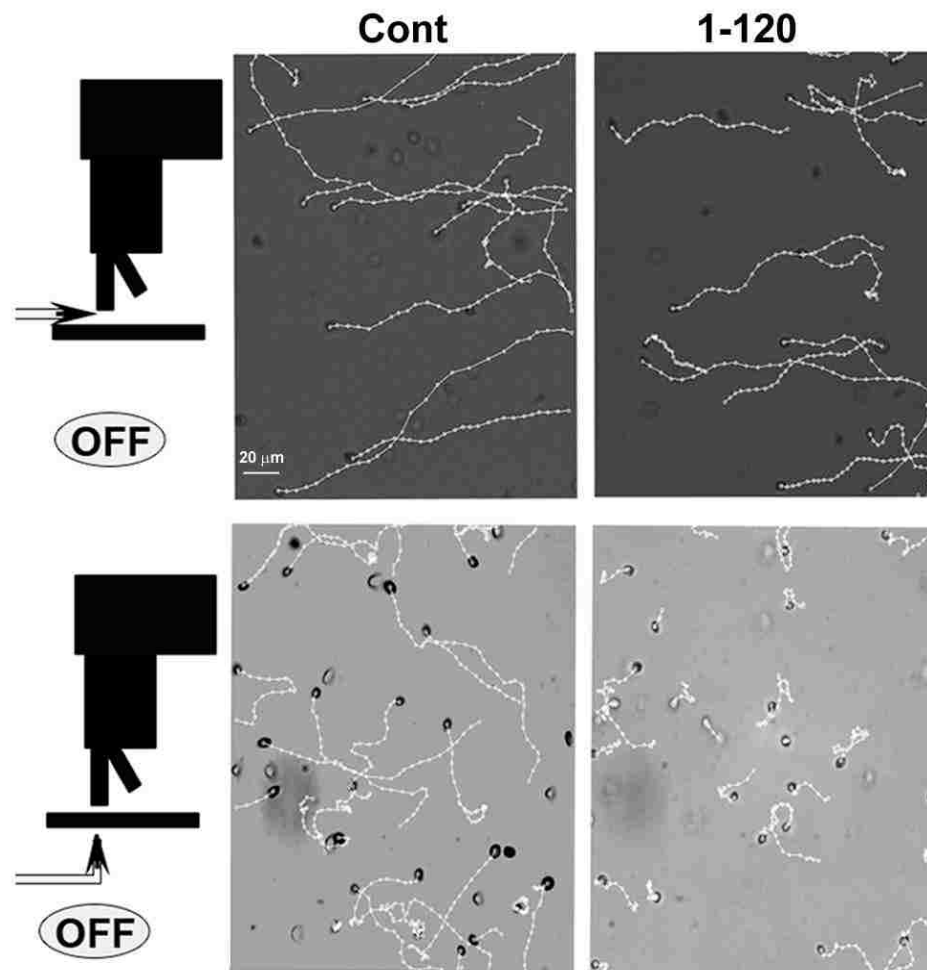


























Figure 4-5. The Irregular Trajectory is Related to the Direction of Light.

Control and RSP2₁₋₁₂₀ (1-120) cells were illuminated with bright light (6 klux) from a fiberoptic of a gooseneck tungsten lamp (arrow). Both strains swam in mostly helical paths when light was parallel to the glass slide (upper panel). The trajectories of mutants became particularly irregular when the fiberoptic was placed vertical to the slide. The light source of the microscope was turned off and the condenser was removed.

4.2.4 Light-Induced Irregular Swimming of Mutant Cells is Calcium-Dependent

To test whether the light-induced irregular motility is calcium-dependent, cells were suspended in growth media which contains calcium, HEPES, HEPES+calcium or HEPES+EgTA as indicated (Table V) and was observed immediately. Control cells swam helically in all solutions and under different light intensities while RSP2₁₋₁₂₀ cells swam helically under dim light in all solutions. Interestingly, the mutants swam helically also under higher light intensity as long as the calcium concentration was low (HEPES or HEPES+EgTA). The irregular movement occurred (under normal light) only when calcium was included in the solution. In the presence of calcium in the media, the incoming calcium usually bound by CaM and CaMB motif of RSP2 may bind to other CaM/calcium binding proteins in this mutant strain. These results suggest the light induced response of RSP2₁₋₁₂₀ cells is calcium-dependent.

Strains	Growth media		Hepes (10 mM)		Hepes (10 mM) EgTA (0.4 mM)		Hepes (10 mM) Calcium (1 mM)	
	D	N	D	N	D	N	D	N
WT								
Cont								
1-120								



Light intensity: D- Dim (~0.1 klux); N- Normal (~1 klux)
Trajectory:  - helical swimming  -irregular swimming

Table VI. Light-induced Irregular Movement of RSP2₁₋₁₂₀ Cells is Calcium-Dependent.

WT, Control (Cont) and RSP2₁₋₁₂₀ (1-120) cells were suspended in growth media or indicated concentrations of Hepes, EgTA and Calcium. Swimming behavior of these cells under Dim (D) and Normal (N) light intensities was observed. WT and control cells swam helically in the presence and absence of calcium while RSP2₁₋₁₂₀ (1-120) cells displayed irregular motility only in the presence of calcium.

4.2.5 Defective Calmodulin-Binding of RSP2 Leads to Irregular Trajectory

The C-terminus of RSP2 has two calcium-dependent CaMB motifs. To test whether the CaMB function of this domain is related to the abnormal phenotype of RSP2₁₋₁₂₀ cells, 2 point mutations were created in the CaMB motif of RSP2. A CaMB* construct was created in which two arginine residues in the positively charged 2nd CaMB motif were replaced with glycine (R581G and R584G). These residues were mutated to reduce the positive charge in the amphipathic helix of the CaMB motif which is required for CaM binding. This construct was expressed in the paralyzed RSP2 mutant, *pf24*. The motile transformants appeared to swim like control under dim light (Figure 4-7). However, when light intensity was increased to normal, the CaMB* cells displayed irregular movement similar to RSP2₁₋₁₂₀ strains. These mutants resumed helical trajectories as soon as the intensity was decreased (Figure 4-7). These similar phenotypes of CaMB* and RSP2₁₋₁₂₀ mutants suggest that the irregular movement is due to defects in the interaction between CaM and RSP2.

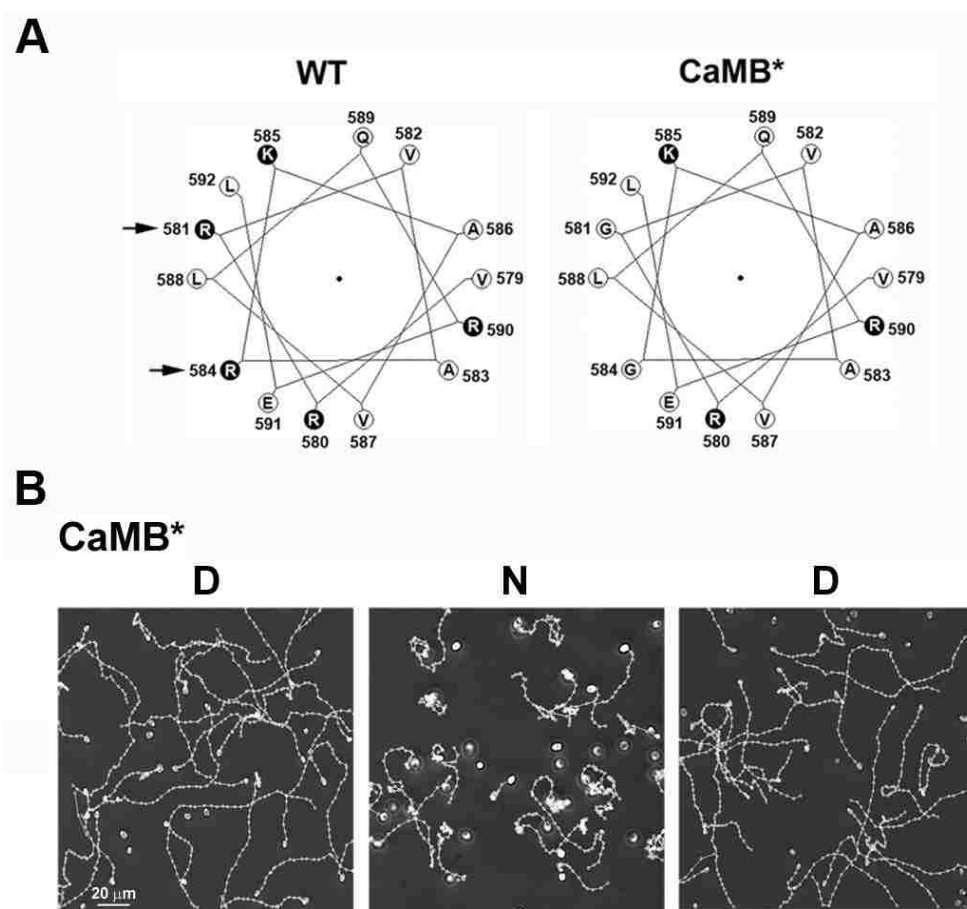


Figure 4-6. Mutants that Express Full-length RSP2 with a Defective CaMB motif also Displayed the Light-induced Irregular Trajectory.

A) Amphipathic helix of the CaMB motif in RSP2. The sequence coding for CaMB motif was subjected to analysis using Helical Wheel Program. The Arginine residues mutated to Glycine in the mutant are highlighted using black arrows. B) Cells expressing the CaMB* construct were observed under a microscope with different light intensities (D ~ 60 lux and N ~ 1 klux). Cell movement was recorded and tracked using Metamorph program. The motility of CaMB* cells was similar to RSP2₁₋₁₂₀ cells and varied with light intensity.

4.2.6 Persistent Light Response of RSP2 CaMB Mutants

To reveal the flagellar movements underlying the irregular trajectories, control and RSP2₁₋₁₂₀ cells were imaged using high speed video microscopy that requires bright illumination (> 20 klux). Control cells (*pf24* rescued with full length RSP2), like typical WT cells, appeared oval in shape and swam at multiple focal planes with synchronized waveform (Figure 4-7A). In contrast, 1-120 mutants were mostly found in a single focal plane near the glass slide. The mutants were found to alternate between swimming with synchronized flagella and oval cell shape or spherical with unsynchronized flagella in which case the cells moved only locally (Figure 4-7A).

A montage of time-lapse images, 1 image every 20 frames (about one of every two beat cycles), shows a typical oval-shaped control cell moving in a curved path (Fig. 4-7B, upper panel). During this movement, the plane of two flagella also rotated around the axis of the cell body. In contrast, the spherical RSP2₁₋₁₂₀ cells did not translocate horizontally (Figure 4-7B, lower panel). The proximal ends of flagella were obscured. The pyrenoid-like granule of the cell (white arrow), which is located opposite to the flagella, appeared near the center of the spherical cell body suggesting change in cell orientation. These images indicated that control cells swam horizontally with the cell body axis parallel to glass, whereas mutant cells switch frequently between vertical (spherical, towards light) and horizontal orientations (oval, away from/ perpendicular to light) as depicted (Figure 4-7B, depicting the relative orientations of cells and viewer/camera). Consecutive images between two frames (arrowheads indicate frame numbers) showed that flagella of a control cell undergo a complete beat cycle (Figure 4-7C, upper panel) while RSP2₁₋₁₂₀ cells turned with asynchronous strokes (Figure 4-7C,

lower panel). Thus the irregular trajectories of the motile RSP2₁₋₁₂₀ mutant cells were likely due to the asynchronous beat and repetitive turning when cells were caught between the perpendicular oriented glass surface and light source.

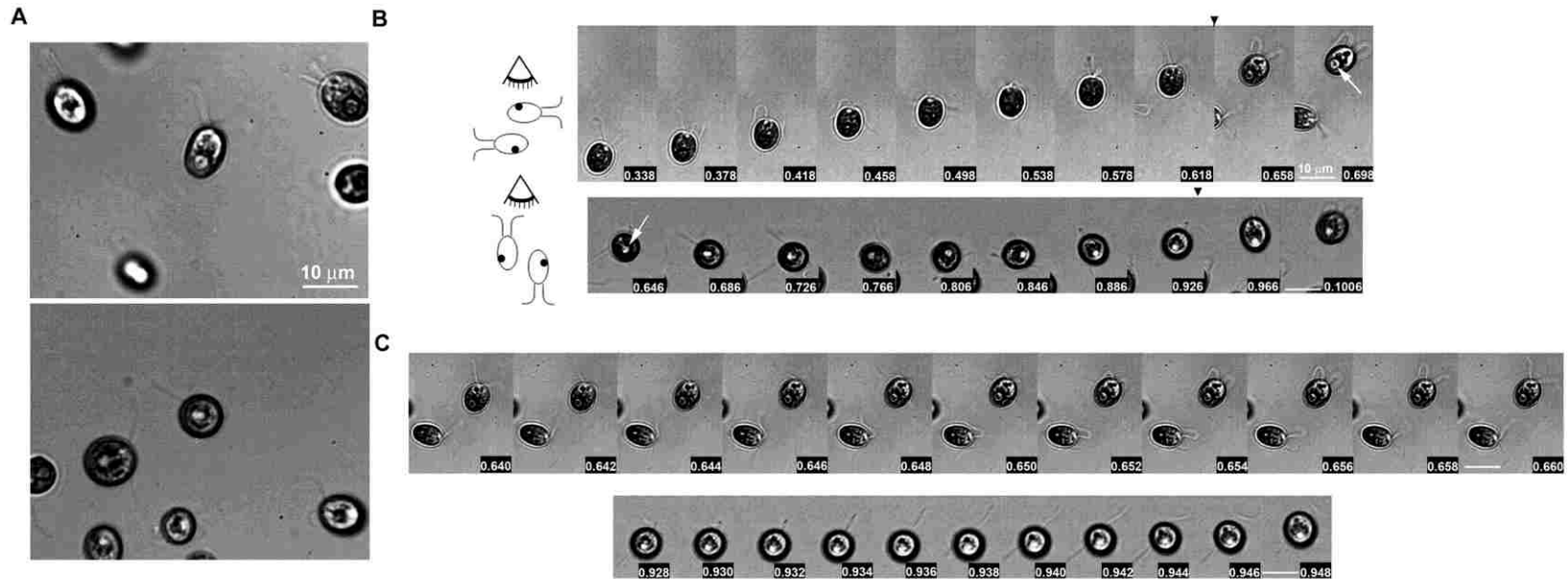


Figure 4-7. Orientation of Cells and Asynchronous Flagella under Conflicting Stimuli.

(A) Control and mutant cells tend to orient differently. A representative image from high-speed video microscopy shows oval-shaped control cells at different focal planes with flagella displaying breast stroke waveform (upper panel). RSP2₁₋₁₂₀ cells often appear circular (lower panel) in a single focal plane near the slide. The proximal ends of flagella are obscured by the cell body. (B) Schematic and montage images compare the orientation and swimming paths. A typical oval WT cell (upper panel) sports synchronous breast-stroke beating flagella, moving in a helical path while rotating along the cell body axis simultaneously. In contrast, mutants appear spherical with two unsynchronized flagella partially hidden by the cell body. The pyrenoid-like granule (white arrow), which is usually positioned opposite to flagella, now appear in the center. Towards the end of the footage, the cell appears oval with synchronized flagella when pulling into a horizontal orientation. The montage was compiled from one per 20 frame images. (C) Consecutive images (between the two frames, arrowheads in B) show a complete beat cycle of the control (upper panel) and a turning mutant cell with two unsynchronized flagella. Light intensity is >20 klux. Time is stamped in seconds.

4.2.7 RSP2 N-terminus Does Not Bind CaM

To test if the truncated RSP2 lost affinity for CaM, four RSP2 recombinant proteins, WT (full length RSP2), CaMB*, truncated a.a. 7-119 and a.a. 7-265 were expressed in bacteria. The truncated proteins were tagged with an N-terminal Maltose Binding Protein (MBP) to overcome low expression and precipitation problems (Donnelly et al., 2006). The sonicated supernatant was incubated with CaM-agarose beads in the presence of 2 mM calcium. Bound proteins were eluted with 2 mM EGTA. Fractions collected before and after incubation with beads were analyzed by western blot. As shown previously, amount of full length RSP2 in the supernatant was reduced after incubation with the CaM-agarose beads (Figure 4-8, compare pre and post of WT) (Yang et al., 2004). CaMB* construct retaining one predicted CaMB site also bound to CaM. In contrast, the two truncated 7-119 and 7-265 polypeptides did not.

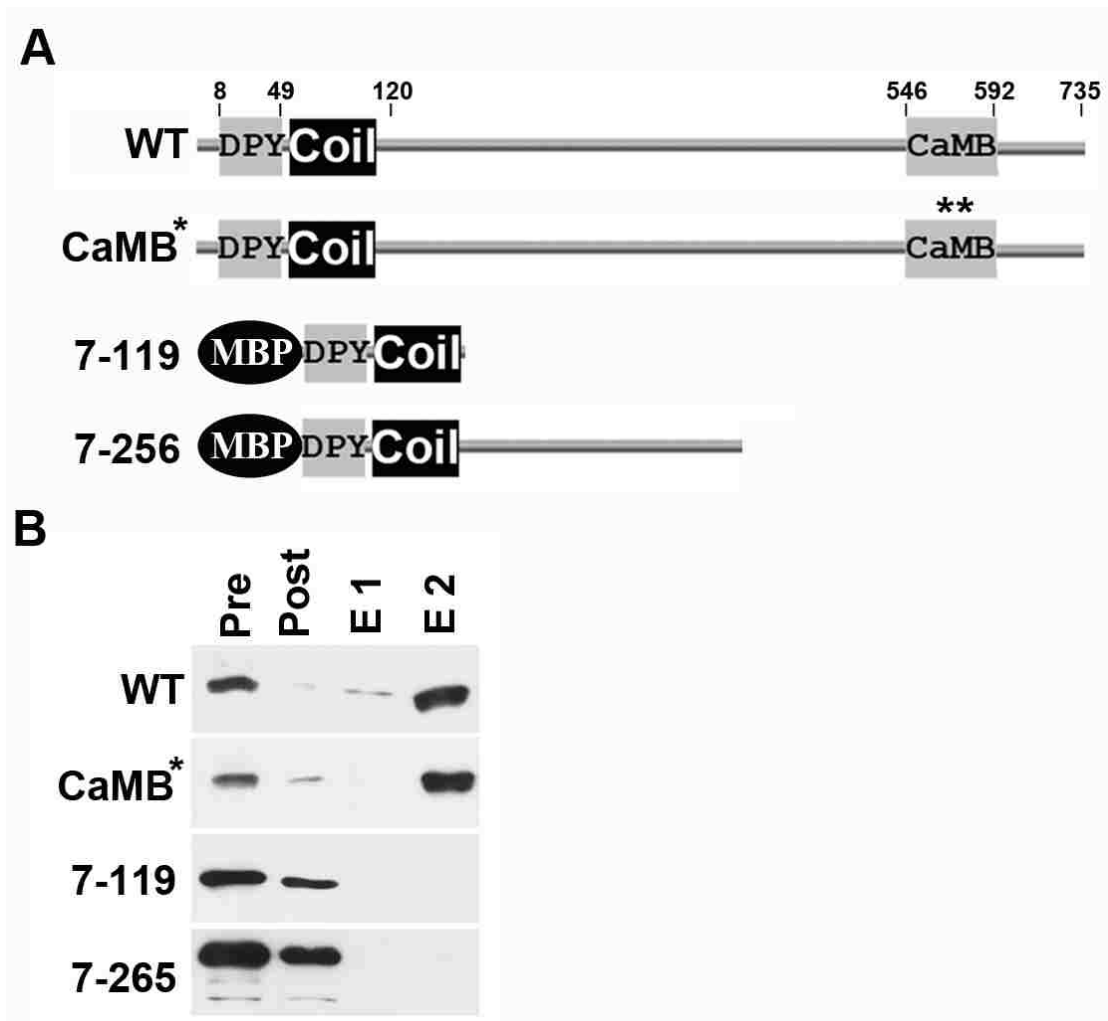


Figure 4-8. Altered CaMB Affinities Due to RSP2 Mutations.

A) RSP2 constructs used for CaM-affinity purification experiments. **B)** Western blot of fractions collected during affinity purification using CaM-agarose beads. Full length recombinant RSP2 and CaMB* bound to the beads in the presence of calcium while the truncated RSP2 mutants (7-119 and 7-265) did not. Pre, bacterial supernatant; Post, flow through; E1 and E2, eluents. RSP2 was revealed by polyclonal antibodies against the purified RSP2₇₋₁₁₉ polypeptide.

4.2.8 Motility and Assembly Deficiencies in RSP2 C-terminus Mutants

To create a tagged RSP2 construct, a 3HA-6His tag was inserted in-frame into an Xho I restriction site in the C-terminus of the RSP2 gene. This approach created a mutant strain (Δ CT-Tag) with a smaller truncation. The stop codon behind the tag sequence terminates the expression, leading to the deletion of the final 16 a.a. of RSP2. The construct was transformed into *pf24* as described in Chapter 2. A similar strategy was taken to create a Δ CT construct in which the tag was absent and 16 a.a. of RSP2 is deleted.

Contrary to the motile RSP2₁₋₁₂₀ strains, most of the clones transformed with the Δ CT-Tag construct were unexpectedly paralyzed like *pf24*. Approximately 3% of the screened transformants contained a mixed population of swimmers and paralyzed cells. The percentages of swimmers dwindled as the liquid culture reached the stationary phase, resembling the existing spoke mutants, *pf25* and *pf26* (Yang and Yang, 2006; Wei et al., 2010). Similar results were obtained from the untagged Δ CT group.

It was demonstrated that the ratio of motile cells of *pf25* and *pf26* strains diminished as liquid cultures progressed into the stationary phase. This deterioration correlated with increased assembly defects in RS and axonemes in general as media became exhausted (Wei et al., 2010). To test if RS assembly of Δ CT-Tag strains was also affected by media, axonemes were harvested from the liquid cultures at different stages for western blots (Figure 4-9). The Δ CT-Tag axonemes from the log phase culture with swimmers and immotile cells appeared similar to control. However, in Δ CT-Tag axonemes from the stationary phase cells that were mostly paralyzed, the two spoke head homologs, RSP4 and 6, were significantly reduced (compare left and right panels in

Figure 4-9). These two spoke head proteins are critical for motility and their drastic reductions accounted for the paralysis of cells in the stationary phase. The short C-terminal deletion may impair the assembly of truncated RSP2 and the spoke head module while these deficiencies exacerbated when media become exhausted.

Thus, the C-terminus of RSP2 likely faces the spoke head and promotes its assembly. Changes in molecular interactions in this region resulted in a range of anomalies in the assembly and the motility.

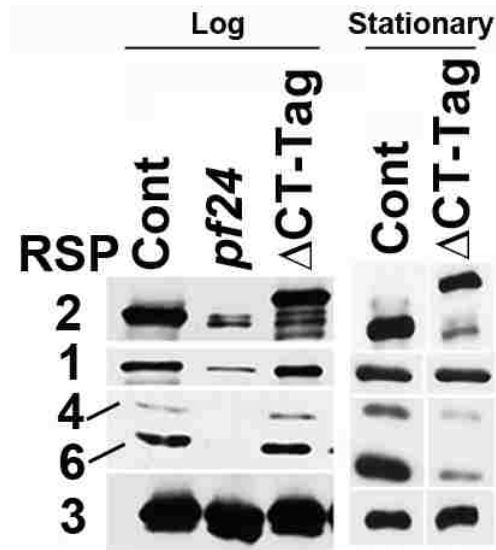


Figure 4-9. Altered Assembly of Spoke Head Proteins in RSP2 C-terminus Mutants.

RS in Δ CT-Tag axonemes prepared from the log-phase culture appeared normal (left panel). However, the spoke head proteins, RSP4 and 6 were reduced if axonemes were prepared from the stationary phase culture in which most of the Δ CT-Tag cells were paralyzed.

4.3 Discussion

These findings support two conclusions. First, the C-terminus of RSP2, although dispensable for flagellar beating, is required to maintain helical swimming under perpendicular orientations of light stimuli and glass barriers. Second, the abnormal motility of RSP2 mutants could be due to defective CaM-RSP2 interaction.

4.3.1 C-terminus of RSP2 may Mediate Steering of Cells Under Conflicting Signals

The normal swimming behavior of RSP2₁₋₁₂₀ cells under dim light suggests that the deleted C-terminus with putative calcium-dependent CaMB motifs is dispensable for flagellar beating. The abnormal trajectory that prevents mutants from leaving the illuminated area suggests that this evolutionarily diverged region may be functional under certain conditions in the environment.

This region is not required for phototaxis since RSP2₁₋₁₂₀ cells without the C-terminus exhibit normal photoaccumulation. However, the irregular trajectories correlated with the orientations and intensity of light indicates that this region is involved in a novel steering behavior. One scenario is that the light sensitive cells, under a regular microscope will swim towards or away from light, inevitably encountering the glass slide or cover slip that is perpendicular to the light beam. This encounter prevents the mutant cells from resuming helical trajectory unless the light intensity is reduced (Figure 4-10).

In contrast, WT cells are capable of exiting this conflicting situation, suggesting that RSP2 C-terminus in the axoneme enables WT cells to ignore the incoming light. This ability could be CaM-dependent since the CaMB* strain in which two residues in the second CaMB motif are mutated also exhibits a similar phenotype.

The inability of RSP2₇₋₁₁₉ to bind calmodulin-agarose supports the prediction that the C-terminus binds CaM.

The fact that control or WT cells can be recorded under high speed video microscopy which requires bright illumination (>20 klux) shows that these cells can swim away from bright illumination without undergoing phototaxis. A typical WT cell with 100 $\mu\text{m}/\text{second}$ velocity and 2 Hz rotation rates (Rüffer and Nultsch, 1985), will take 4 seconds to translocate through a field of 400 μm diameter. During this time, the cell body in theory will rotate 8 times exposing the eyespot repetitively to light. However, WT cells or controls maintain a horizontal trajectory under these conditions as shown in a 2 second (1000 frames) recording. They do not turn towards light. Together these observations suggest that WT cells under these circumstances are not responding to light as expected for phototactic cells. In contrast, the appearance of mutant cells alternating between circular (with asynchronous flagella strokes) and oval (with synchronous strokes) cell shapes suggest cycles of turning towards and away from light and glass surface resulting in irregular trajectories (Figure 4-10).

Thus the RSP2-CaM interaction in WT cells may serve as an inhibitory mechanism which allows cells to switch off light response and swim away from conflicting signals in natural environments.

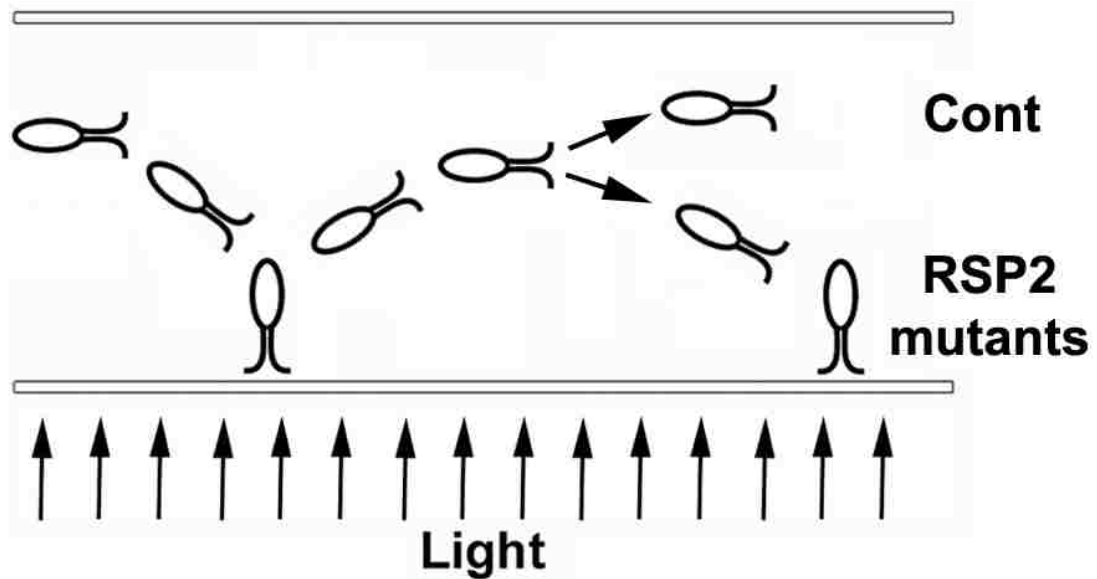


Figure 4-10. Schematic Depicts the Movement of Control and RSP2 mutants from High Speed Video Microscopy Images.

Motile cells of either type (on the left) turn towards light penetrating through the glass. WT cell turns again and maintains a horizontal orientation swimming away from light while mutants, defective in CaM-binding, turn towards light and glass repetitively.

CHAPTER V. ROLE OF NDK DOMAIN IN RSP23

5.1 Introduction

The presence of a Nucleoside Diphosphate Kinase (NDK) in the RS is intriguing. In fact, the spoke NDK, RSP23, was discovered accidentally during a search for flagellar NDK (Patel-King et al., 2004). It is homologous to the mammalian protein, NDK-5 (Figure 5-1A). Although recombinant NDK-5 in bacteria precipitated and exhibited no enzymatic activity (Munier et al., 1998), WT flagella displayed higher NDK activity than the spoke-less ones.

In addition to the NDK domain, RSP23 contains interesting features related to RSP2, a spoke protein responsible for linking the spoke head to the rest of the spoke and involved in steering control (Chapters 3 and 4). First, the assembly of RSP23 is dependent on RSP2 (Patel-King et al., 2004). In the RSP2 mutant, RSP23 is diminished, suggesting it is located near the spoke head (Huang et al., 1981). Secondly, both RSP2 and RSP23 have a DPY-30 domain. This Dimerization/Docking (D/D) DPY-30 domain found in RSP2 is critical for proper association of RSP2 and spoke head in the RS complex and thus for flagellar beating (Chapter 4). Thus, contrary to other NDK's that function as trimers or hexamers (Lascu et al., 2000), NDK in RSP23 may operate as a dimer due to the presence of the DPY-30 domain and may have a targeting mechanism similar to RSP2.

In addition, both molecules contain CaMB motifs in the extended C-terminus that are absent in their mammalian homologs. The C-terminal 1-8-14 CaMB motif in RSP2 maintains steering of cells amidst conflicting signals whereas RSP23 has IQ motifs,

whose function is not known. The IQ motifs are another class of calmodulin binding motifs and conform to the (I/V/L)QXXX(K/R)XXXX(K/R) consensus (Rhoads and Friedberg, 1997). The 2 types of CaMB domains in these proteins could be involved in a similar function: motility control. Alternatively, the IQ motifs in RSP23 may modulate NDK activity (Patel-King et al., 2004). The question is why the RS which functions as a mechanochemical transducer contains such an enzyme.

NDK is ubiquitously found in organisms from bacteria to humans. The enzyme is known to catalyze transfer of a phosphate group from a Nucleoside TriPhosphate (NTP) to a Nucleoside DiPhosphate (NDP). The conversion maintains the equilibrium of nucleotide species in the nucleus as well as in the cytoplasm. This enzymatic domain is present in many molecules in different molecular contexts. In fact there are 9 human NDK. Based on sequence similarities, human NDK are further divided into two groups. Group I has 4 members (NDK 1-4) which are highly similar to each other and expressed ubiquitously. NDK 1 and 2 are best characterized. They are implicated in metastasis suppression and they are less abundant in highly metastatic cancers (reviewed in Lombardi et al., 2000).

Members of Group II (NDK 5-9) are more divergent among themselves than Group I. They vary in their length and associated domains. Some of them contain consecutive NDK repeats or other domains (Lacombe et al., 2000). For example, NDK-5 members are usually ~212-a.a. long. Proteins homologous to NDK-5 are found in several species ranging from mammals to *Chlamydomonas*. The *Chlamydomonas* homolog of NDK-5, RSP23, has a longer C-terminus (~374 a.a. longer). The unique feature of NDK-5 members is a C-terminal DPY-30 domain (Figure 5-1A). Human NDK-5 is moderately

expressed in several tissues while being most abundant in the adult testis.

Immunolocalization studies showed that NDK-5 is present along the sperm flagella, specifically near the CP microtubules (Munier et al., 2003).

The catalytic mechanism of NDK resembles the two-component prokaryotic histidine kinase (Almaula et al., 1995). An evolutionarily conserved histidine residue in the NDK domain (H121 in *Chlamydomonas*) obtains a phosphate group from a Nucleoside TriPhosphate (NTP) donor during the catalysis. The phosphate in this unstable intermediate is quickly transferred to nearby acceptors such as Nucleoside DiPhosphates (NDP) to produce a triphosphate molecule (Figure 5-1B and C). Through this mechanism, the equilibrium of different nucleotide species can be maintained.

Flagella require different nucleotide species, especially ATP and Guanosine TriPhosphate (GTP). ATP is required to fuel the high frequency oscillatory beating powered by numerous axonemal dynein ATPases. Furthermore, the periodic interaction of RS with CP and rotation of CP microtubule during flagella beating may also require ATP. It has been speculated that an ATPase present in the spoke head drives the CP rotation during oscillatory beating (Ogawa and Gibbons, 1976). It is now known that the spoke head does not contain any ATPase. However, an NDK in the RS that generates ATP for the kinesin ATPase found in the CP may be in line with this prediction.

NDK may contribute ATP for the assembly of RS in flagella. A spoke HSP40 located near NDK is added into the RS complex at a later stage in the assembly of RS (Yang et al., 2005). It remains unknown if the flagellar HSP70 ATPase is involved in this late addition. In the cell body, HSP40 and HSP70 work together as molecular chaperones for protein folding. If this is true, an NDK in the vicinity providing ATP may

be critical for the assembly of the spoke HSP40 that is in turn necessary to support synchronized flagellar beating.

ATP is also required for the IntraFlagellar Transport (IFT) process that is driven by kinesin and cytoplasmic dynein (Rosenbaum and Witman, 2002). IFT shuttles components required for flagellar elongation and maintenance between the cell body and flagellar compartment. The IFT train that transports cargo is a multisubunit complex.

The need for energy throughout the length of the flagella is evident. However, the supply mechanism is only partially understood and is complicated. For example, ADenylate Kinase (ADK) and enolase that are involved in the ATP generation pathways are associated with the CP complex. Mutations in these genes cause reduced beat frequencies and flagellar ATP concentrations (Zhang and Mitchell, 2004; Mitchell et al., 2005). ADK and enolase belong to a subcomplex in the CP that contains guanylate kinase and HSP70. Subunits of outer dynein arms are also associated with ADK activity (Wirschell et al., 2004). RSP23, the spoke NDK (King et al., 2004), may be one of the enzymes in this ATP generation network.

Alternatively, NDK could convert ATP to GTP in flagella. The role of GTP in flagella is not yet clear but is likely important. An IFT subunit, IFT27, is a small GTPase (Qin et al., 2007). RNAi mutants of IFT27 were defective in flagellar generation and mitosis.

The aim of this study is to elucidate the role of NDK domain (of RSP23) in flagella. To test if the NDK domain of RSP23 plays a role in these NTP-dependent events in flagella, this pilot study generated mutant strains that express enzymatically inactive

spoke NDK. The preliminary analysis of phenotypes suggests that the enzymatic activity of spoke NDK has multiple roles.

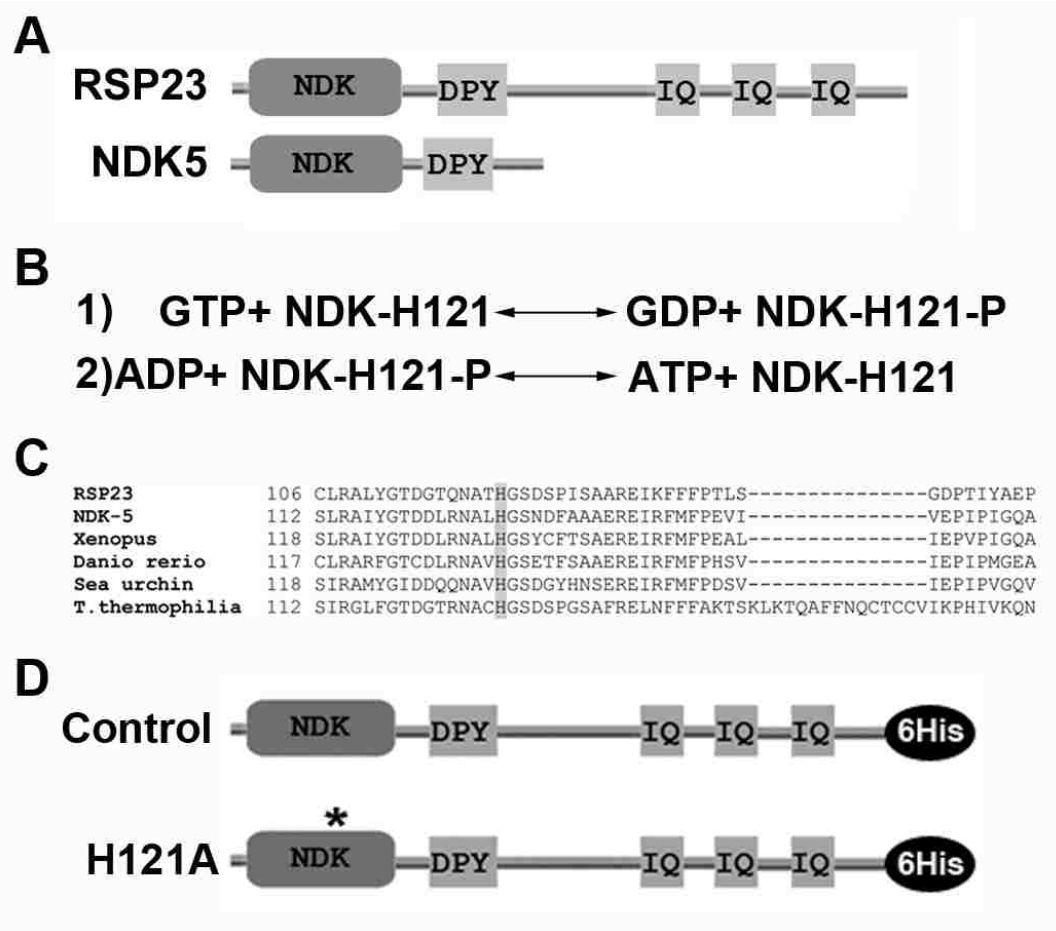


Figure 5-1. Molecular Domains, Catalytic Mechanisms and Mutation Constructs of NDK (RSP23).

A) Molecular domains in *Chlamydomonas* RSP23 and Human NDK5. Only the N-terminus (NDK and DPY-30) is evolutionarily conserved. **B)** Mechanism of triphosphate generation by NDK. H121 is transiently phosphorylated during catalysis. **C)** Sequence alignment around the region containing the catalytic histidine in NDK5 homologs including *Chlamydomonas* RSP23 and Human NDK5 **D)** Tagged control and histidine mutant construct to be expressed in WT cells. The His tag will distinguish the exogenous molecules from the endogenous RSP23.

5.2 Results

To test the role of spoke NDK, the strategy is to express RSP23 with inactive enzyme. However, it is not possible to generate an RSP23 mutant strain because targeted gene mutagenesis in *Chlamydomonas* is not yet feasible and RSP23 mutants from random mutagenesis have not been recovered. Currently, the only option is to express the dead enzyme in the wild type background. If NDK activity is not required for its assembly, both inactive and active enzymes will be assembled into the RS complexes.

If the spoke NDK provides ATP for axonemal dyneins, the strain expressing inactive NDK will have reduced swimming velocity. If it mediates the assembly of HSP40 or RS, the mutant flagella will display a spectrum of motility defects, ranging from twitching flagella like HSP40 mutants (Yang et al., 2008) or paralysis like spoke-less flagella (Huang et al., 1981). If the nucleotides are used for IFT, NDK mutants may have short or no flagella. If nucleotides are for the assembly of axonemal complexes, the flagella could be normal or short, depending on how many complexes are affected, while the affected axonemal complexes will be in reduced amounts.

Toward this goal, two 6His-tagged constructs (Control and H121A) were generated (Figure 5-1D). To create these constructs, the promoter for flagellar LC8 gene was used. LC8 is a very abundant protein in flagella and the gene does not contain any intron. The rationale is to use the powerful LC8 promoter to drive the expression of NDK. Furthermore, the plasmid carrying the LC8 promoter also contains a PMM-resistant cassette to aid in selection (Yang et al., 2009). For generating the control, the entire RSP23 cDNA was cloned into the LC8 plasmid to replace the LC8 cDNA. This construct was then used as a template for site-directed mutagenesis to replace Histidine

(H121) to Alanine. Previous studies have demonstrated that this residue in other NDK's transiently receives the phosphate during the catalysis and mutation of this residue abolished the enzymatic activity (Tiwari et al., 2004; Dumas et al., 1992). These two constructs were transformed into WT *Chlamydomonas*.

Approximately, 300 colonies for each construct were recovered from 3 independent transformations. To identify the transformants expressing NDK in the axoneme, 25 clones from each group (Control and H121A) were randomly selected to prepare crude flagella. Western blots of the flagella preparation were probed for the presence of the 6His tag. Four His-positive clones from each group were selected for further analysis (Figure 5-2).

5.2.1 NDK Mutants have Shorter Flagella

The His-positive strains were cultured in liquid media and observed daily after inoculation. The control strains expressing tagged full length RSP23 had full length motile flagella (10-13 μm). In contrast, the flagella from the four mutant strains which expressed inactive NDK were shorter. The flagella of #1, 3, and 4 strains were half or three-fourth length (Figure 5-3A and B) and mostly paralyzed. WT flagella of such a length would have been motile, suggesting that mutants may have additional biochemical deficiencies in axonemes. The flagella of clone #2 were motile and slightly longer. The length of flagella did not increase throughout the light cycle. The shorter flagellar length suggests that NDK activity of RSP23 is at least important for flagella elongation.

5.2.2 NDK Mutants are Defective in RSPs

To assess the assembly of RS complexes, axonemes isolated from control and H121A mutants were analyzed using western blots (Figure 5-4). Total RSP23 was revealed by anti-RSP23 while the His-tagged NDK from the introduced construct was revealed by anti-His antibody. All samples contained the His-tagged NDK. However, the total amounts of RSP23 from the H121A strains appeared lower. Spoke proteins RSP3 and RSP16 were also less abundant. In contrast, outer dynein arms, represented by the Intermediate Chain, IC78 (used as loading control), were indistinguishable. This result suggests that the assembly of the entire RS complex is compromised in H121A strains.

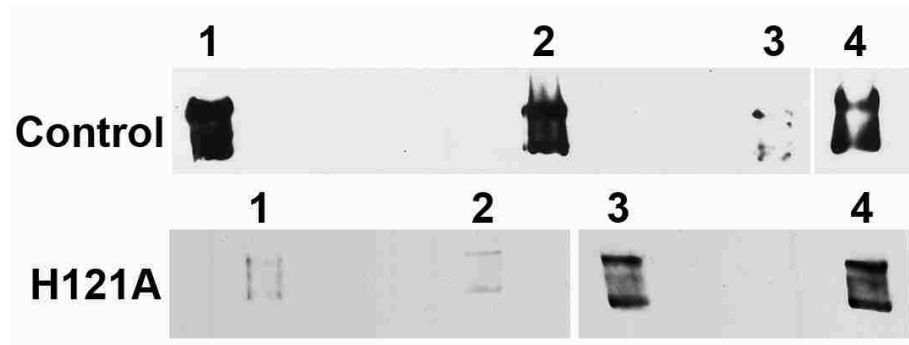


Figure 5-2. Representative Western Blots of Flagella from Clones Transformed with Control or Mutant NDK Tagged Constructs.

The blots were probed for anti-His antibody. Note the samples were from crude flagella preparations primarily for the detection of positive clones and are not quantitative comparisons.

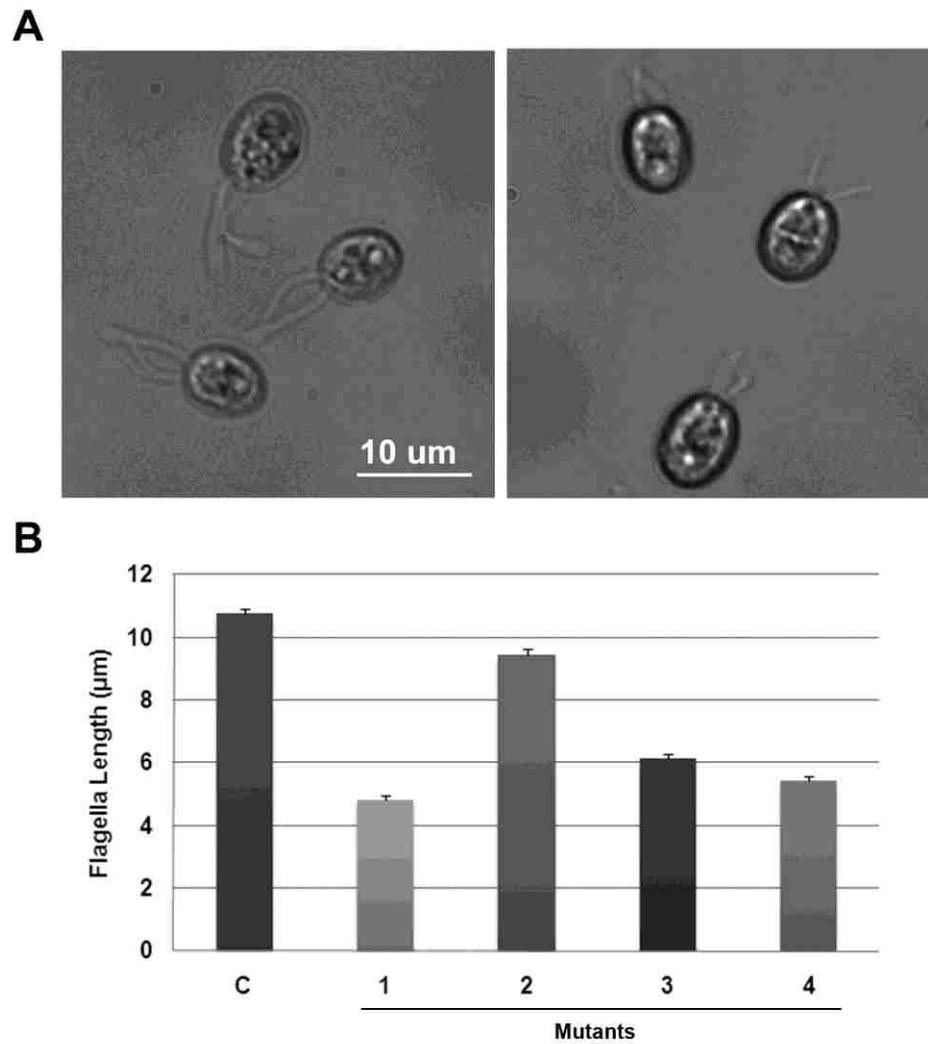


Figure 5-3. Inactive NDK Mutants have Shorter Flagella.

A) Control and mutant strains (1-4) cultured in liquid media. Montage images show full length flagella of Control cells (left panel) and shorter flagella of mutants (right panel). **B)** The histogram of flagella length. The data was calculated and plotted using ImageJ software. N=50.

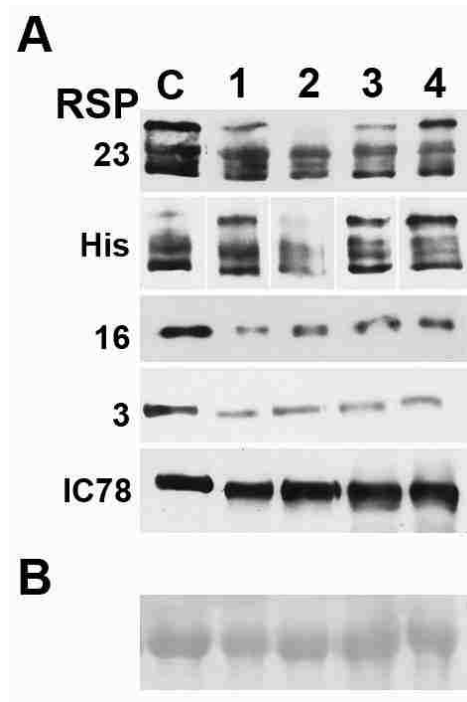


Figure 5- 4. RS Complex is Less Abundant in the Axonemes of Inactive NDK Mutants.

A) Axonemes extracted from Control (C) and mutants (1-4) were analyzed by western blot and probed for representative RSPs, His and IC78. The levels of RSP16 and 3 were reduced. **B)** Ponceau-stained blot of tubulin in the axoneme to show loading levels.

5.3 Discussion

This pilot study perturbing the activity of spoke NDK revealed encouraging preliminary data. First, both His-tagged active and inactive NDK were incorporated into the RS complex. Thus the His-tag does not interfere with the assembly, indicating that this strategy of co-expression is, indeed, feasible.

Secondly, partial replacement of active RSP23 with an inactive form correlates with shorter flagella and reduced RS assembly. The reduction of RS complex is consistent with the paralysis of shorter flagella.

Although these results are preliminary, there are several possible interpretations. NDK activity may be important for the assembly of RS complexes. RS including RSP2 is partially assembled in the cell body into a precursor complex first. The reduction in the overall RS amount could reflect the reduced assembly of the precursors, transport or the conversion of the precursor into the axonemal RS. In addition, NDK activity may be involved in flagellar elongation, either by promoting IFT or the assembly of other axonemal complexes except outer dynein arms. It is possible that these phenotypes are artifacts due to over-expression driven by the LC8 promoter. LC8, which is important for flagellar elongation and assembly of multiple axonemal complexes, could be reduced or displaced in these mutants. This scenario seems unlikely since the control strains did not exhibit these phenotypes and four independent isolates shared similar phenotypes albeit of slightly different severity.

These possibilities could be clarified by further experimentation. First of all, more transformants, for both control and inactive groups, should be analyzed. Secondly, the amounts of LC8 and the His-tagged proteins in the cell body should be examined.

Furthermore, an independent approach should be taken to knock down active NDK. This can be achieved by knock down of NDK expression with RNAi (Yang et al., 2008) and miRNA (Zhao et al., 2008). These approaches were successfully applied to knock down certain *Chlamydomonas* genes (DiPetrillo and Smith, 2010). However, the success rates are low and the phenotypes are not often stable. An alternative approach is to use another model system, such as zebrafish that is more amenable for gene targeting. Morpholinos have been used to knock down the level of spoke head proteins in zebrafish (Castleman et al., 2009) and only motile cilia in the knockdown fish were defective. If the phenotypes in these NDK mutant strains are correct, injection of NDK-5 morpholino will also result in paralyzed and possibly shorter or no cilia. If NDK-5 is involved in IFT, both sensory and motile cilia will be affected. These animals with significant knockdown of NDK-5 may display situs inversus and cystic kidney.

CHAPTER VI. DISCUSSION

The investigation of the two DPY-30 domain containing proteins present in the RS of *Chlamydomonas* sheds new insight on this domain, the RS complex and flagellar mechanisms.

6.1 The Conserved RSP2 N-terminus Functions as a Bivalent Structural Linker

Although RSP2 is 735-a.a. long, RSP2₁₋₁₂₀ that contains the DPY-30 domain trailed by a coiled-coil not only restores the RSPs but also rescues the paralysis of the RSP2 mutant, *pf24* (Figure 3-5 and Figure 4-2, left panel). Thus, the N-terminal conserved region is sufficient for the basic function of RSP2 and the short mammalian proteins like DYDC2 are likely to be orthologs of RSP2. Since Δ DPY-30 also restores defective RSPs, the helix downstream to the DPY-30 domain may be involved in the assembly. The DPY-30 domain is important for the RS structure since these restored RSPs are not assembled properly as evident by the paralyzed flagella and the dissociation of truncated RSP2 from the spoke base and other RSPs in the KI buffer (Figure 3-6). Preliminary evidence from the lab suggests that the binding partner of DPY-30 domain is RSP3 which is a dimeric spoke stalk protein.

Based on these results, homodimerization of the DPY-30 domain (Dong et al., 2005) and other dimeric components in the RS, it is proposed that the dimeric RSP2₁₋₁₂₀ functions as a bivalent structural linker for linking the spoke head module to the stalk (Figure 6-1). The dimeric DPY-30 domain (grey circles), works like the D/D domain of RIIa and may recognizes RSP3 in the spoke stalk (black and grey wires represent RSP3 monomers). The binding may promote the trailing helices (rectangular bars, middle

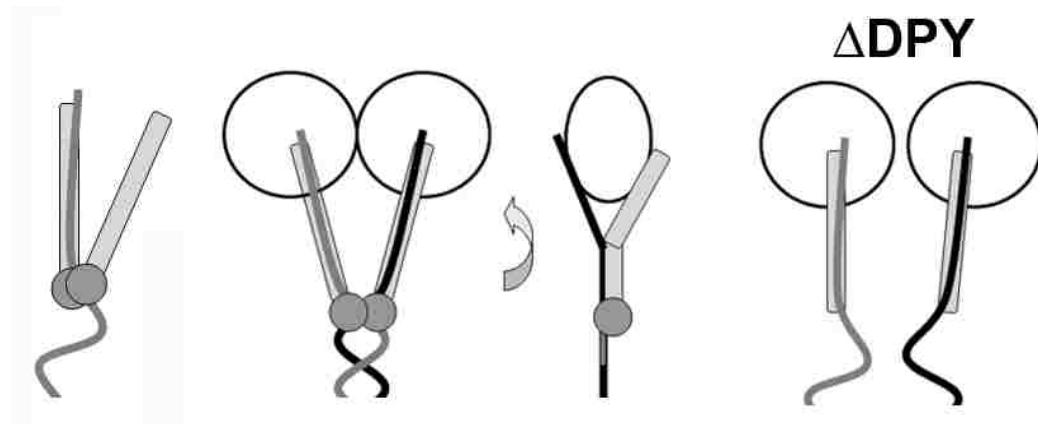


Figure 6-1: Model Illustrating Role of RSP2 Conserved Region in Assembly of RS and Motility.

DPY-30 dimer (grey circles) docks structural motifs (grey rectangles) in RSP2 to the RSP3 monomer (wires) and guides the flanking sequences to form coiled coils and stabilize RSP3 (left panel). The four polypeptides then recruit the two spoke head homologs (clear circles, see second panel and 90° view in third panel). Without the DPY-30 domain (right panel), the dimeric platform is uncoupled, leading to paralyzed crossed flagella. The DPY-30 domain containing RSP23 is not illustrated for clarity.

panel) to form coiled coils with specific regions in RSP3 and possibly other RSPs, namely RSP16 (HSP40) and RSP23 (not shown) in the stalk and the paired spoke head homologs (large clear circles) (Yang et al., 2006). This interaction at the head-neck junction is critical for the coupling of CP and the outer doublets. Without the DPY-30 domain (right panel), these RSPs cannot operate as a functional unit during RS-CP transient engagement. Consequently, these molecules, although present, may wobble, and fail to couple the rotating CP to the sliding outer doublets effectively. Such a faulty machinery leads to stalling, reverse bend formation and crossed flagella, as shown by the flagella of Δ DPY-30 strain (this study) and HSP40-minus strain (Yang et al., 2009).

6.2 The C-terminus of RSP2 with the CaMB Region Modulates Spoke Head and the Photoresponse.

The extended 600 a.a. C-terminus of RSP2 appears dispensable. This region is absent in most organisms while *Chlamydomonas* cells without this region are motile. However, mutation in this region reduced spoke head stability in KI buffer and caused a light-dependent motility phenotype. Similarly, deletion of the last C-terminal 16 a.a. of RSP2 also lead to variation in the level of spoke head proteins depending on the culture conditions. The amount of spoke head proteins is normal in flagella from the log-phase culture but dwindles in the stationary phase. These results suggest that the N-terminus of RSP2 orients towards the spoke stalk while the C-terminal end is near the spoke head, capable of affecting the assembly or conformation of the spoke head.

This effect on the spoke head region confers on the biflagellate *Chlamydomonas* an ability that was not recognized previously. The motile strains with mutations in the C-terminus, either RSP2₁₋₁₂₀ or CaMB*, swim in helical trajectories like WT under dim

light. However, the swimming path turns irregular under bright light that is perpendicular to the glass surface. The irregular path appears to stem from repeatedly swimming towards and away from light and the glass. In contrast, control or WT cells swim horizontally between the glass surfaces, although the eye spot is positioned to sense the light (Figure 4-10). With a normal C-terminus in RSP2 that can interact with CaM, these cells seem temporarily unresponsive to light.

Based on these results, it is postulated that CaM-RSP2 functions as a regulatory switch upstream to phototaxis (Figure 6-2). WT cells under a microscope initially swim towards the light source. However, upon encountering the obstructing glass surface, a calcium surge may occur. The increase in calcium may change CaM-RSP2 interaction, altering the conformation of the spoke head and its interaction with CP. This subtle modification in the RS does not paralyze flagella but is sufficient to prevent WT cells from turning towards light prior to the termination of this refractory period when calcium is pumped out. In contrast, RSP2 with the mutated C-terminus cannot switch off phototaxis and continually swim towards the light and into the glass surface. This model explains the fact that it is possible to observe/record the remarkably light sensitive *Chlamydomonas* without a filter under a bright field microscope. Such a transient modulation allows the algae to swim away quickly from conflicting signals in natural environments. Since phototaxis also requires calcium, the opposing effects of calcium on phototaxis may be achieved by different concentrations, locations or timing and distinct calcium sensors.

The RS is indirectly implicated in phototaxis. Two flagella must generate different output in order to change swimming directions (Kamiya and Witman, 1984;

Rüffer and Nultsch, 1995). One of the key targets of the RS is a subunit of the inner dynein arm known as I1 (Porter and Sale, 2000). The I1 inner arm complex (also known as the f dynein complex) is a two-headed isoform composed of two heavy chains (1-alpha and 1-beta), three intermediate chains and three light chains. The I1 subunit occupies a specific position proximal to the first radial spoke and repeats every 96 nm along the length of the axoneme (Piperno et al., 1990). It was proposed that the RS suppresses the phosphorylation of inner dynein subunit, IC138. Several I1 mutants that hyper-phosphorylated IC138 or with defects in I1 motor, display weakened phototaxis and flagellar bend of reduced amplitude (Habermacher and Sale, 1997; King and Dutcher, 1997; Kamiya, 2002; Okita et al., 2005). When the eye spot senses light, the signaling is transduced differentially in cis- and trans- flagella that are positioned slightly different from the eye spot (Okita et al., 2005; Iomini et al., 2006). The differential signaling may ultimately act on I1 to alter the bend amplitude in one flagellum more than the other. Calcium-induced changes in CaM-RSP2 in the RS may block the formation of differential bend amplitude by affecting I1 and thus preventing WT cells from turning to light transiently.

RSP2 that allows *Chlamydomonas* to steer amidst the conflicting stimuli is another example for control of simultaneous signaling (Coba et al., 2009). This example shows that steering mechanisms are much more complicated than currently recognized. Many calcium- and calmodulin- binding proteins in axonemes (Casey et al., 2003; Patel-King et al., 2004; Dymek et al., 2007) may be actively involved in the control of steering. The calcium- or calmodulin- binding proteins may respond concertedly when the calcium concentration changes to fine tune RS/CP control system. In addition, changes in the RS-

CP control system and in dynein motors (Smyth and Berg, 1982; Sakato et al., 2007; Wakabayashi et al., 2009) may be coordinated. The integrated calcium-sensing system built into the axoneme could potentially alter motility parameters in various ways, such as the pitch, radius or rotation rate of the helical trajectory (Kamiya and Witman, 1984). The mechanisms modulating these parameters remain largely unknown.

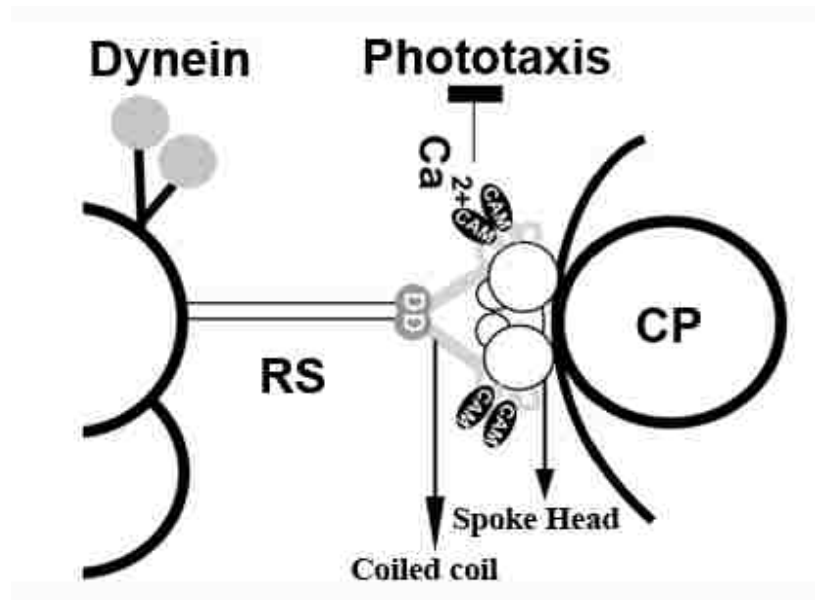


Figure 6-2: Model Elucidating Role of CaMB Domain of RSP2.

Calcium binds to CAM-RSP2 and this alters RS-CP interaction to modulate phototactic turning. Conformation changes in spoke head and CP may affect dynein arms to temporarily switch off phototaxis in control and WT cells making them irresponsive to light. Only part of the 9+2 axonemes is illustrated for clarity. D –DPY-30 domain of RSP2; CAM –Calmodulin.

6.3 NDK Activity of RSP23 may be Important for the Assembly of the RS Complex and Flagella length.

The study of RSP23, the spoke NDK, is exploratory due to the technical limitations in *Chlamydomonas*. However, the results from mutants co-expressing RSP23 with and without enzymatic activity are encouraging. Expression of mutated NDK (H121A) correlates with reduced levels of RSP16 and RSP3, suggesting that inactive NDK perturbs RS assembly and that the inactive gene is co-dominant. Interestingly, the flagellar length of these strains is shorter as well. The shorter flagella are not likely to be transformation artifacts. Such a phenotype has never been observed before in numerous transformations that have been performed in the lab. This raises the prospect that this spoke NDK may actually play a role independent of RS and flagellar motility. This broader role is supported by the EST profile of human NDK-5 from tissues that do not have motile cilia and flagella (NCBI EST database).

NDK may provide nucleotides for flagellar elongation. Most axonemal components are transported into the flagellar compartment as prepackaged precursor complexes. At the tip of flagella they are further modified and assembled into the axoneme (Johnson and Rosenbaum, 1992; Yang et al., 2005). NDK may provide ATP for the ATPase HSP70 chaperone enriched at the tip of the *Chlamydomonas* flagella for protein folding during the assembly process (Bloch and Johnson, 1995). Consistently, HSP70 and NDK co-expressed in *E.coli* and human cell lines co-purify (Leung and Hightower, 1997 and Barthel et al., 1999). Alternatively, NDK may provide nucleotides, either ATP or GTP for IFT. Once, flagella reach full length, IFT still continues for

maintenance. The abundance of nucleotides may ultimately determine the length of flagella.

This interpretation is not contradictory to the full length flagella of spokeless mutant, *pfl4*. It is possible that RSP23 is transported separately from the RS precursor and thus the entry of RSP23 into flagella is independent of entry of RS complex. Once flagellar elongation is completed, NDK may dock to the RS via the DPY-30 domain. At this position, NDK may become one of the players in an ATP/NTP producing network along with enolase and adenylate kinase in the CP (Zhang and Mitchell, 2004).

These preliminary results and predictions can be tested further in the future. The mutant flagella should be tested for the reduction of NDK activity. To investigate if RSP23 is part of the precursor complex, detergent-soluble membrane-matrix components can be extracted from WT and *pfl4* for sucrose gradient sedimentation. Finally, RSP23 knockdown can be achieved by miRNA. It may be more conducive to knock down NDK-5 in a different model system, such as zebrafish, in which knockdown is much more reliable.

6.4 The Role of RIIa Superfamily

RSP2 and RSP23 are only two of the nearly 400 members in the RIIa superfamily. Until this study, the roles of the other members remain largely unknown except for anchoring of PKA. RSP2 is critical for the assembly of radial spoke structural complex while NDK activity in RSP23 seems important as well. These results strongly suggest that the functional mechanism of this superfamily is much more diverged than anchoring of components in the cAMP-dependent pathway (Table III and IV).

Nucleotide metabolism seems to be a major mechanism targeted by these D/D domains. In addition to NDK-5, the D/D domain is also found in several adenylate kinases (ADK) (Table IV and PFAM database). The flagellated protozoan parasite, *Trypanosoma brucei* has seven ADKs isoforms. Two of them (ADKA and ADKB) have an N-terminal extension of ~55 a.a., which is necessary and sufficient for targeting these molecules into the flagellar compartment (Pullen et al., 2004). Our visual inspection shows that these N-terminal extensions are actually highly homologous to the DPY-30 domain, although they are not yet included in the PFAM RIIa superfamily database. Thus, this superfamily is likely larger and one of the functions that are targeted by the two RIIa clan domains may be enzymes for nucleotide metabolism. The localization of such functions may ensure that the needs of nucleotides are met locally.

The D/D domain likely also target structural domains. This new concept underscores the importance of precise assembly of structural complexes. The structural role of RSP2₁₋₁₂₀ in the RS complex may be applicable to some RIIa superfamily members that do not contain any conspicuous domains. For example, the dispensable RIIa protein, RSP11 that prevents paralysis of *Chlamydomonas* flagella in a nutrient-deprived environment (Yang and Yang, 2006; Wei et al., 2010), may simply strengthen RS structurally.

Likewise, DPY-30 in *C.elegans* may play a similar structural role in diverse complexes. It is a small subunit in the core of chromosome modification complexes in diverse organisms (Lieb et al., 1996; Nagy et al., 2002; Cho et al., 2007). It is present in the nucleus of *C. elegans* at all developmental stages (Hsu et al., 1995). It is essential for the localization of a chromosome condensation protein, DPY-27, to the X chromosome

(Chuang et al., 1996) and for the dosage compensation machinery. Defective DPY-30 gene results in XX-specific lethality and various developmental abnormalities in XO nematodes. Similarly, yeast DPY-30 homolog, Sdc1, is an important component of the eight-member histone 3 lysine 4 (H3-K4) methyltransferase (HMT) complex (SET-1 protein complex) (Nagy et al., 2002). Mutations in DPY-30 (Sdc1) or its binding partner Bre2 results in global H3K4 methylation defects and decreased gene expression (South et al., 2010). In the mammalian system, DPY-30 and its binding partner ASH2L (Bre2 homolog), along with other conserved proteins constitutes a sub-complex that is found in all human Set-1 like HMT complexes (Cho et al., 2007). The core of this nuclear complex is also involved in endosomal trafficking in the Golgi apparatus (Xu et al., 2009). Contrary to this broad expression pattern, DPY-30L2, a DPY-30 homolog in *Drosophila* is expressed only in larval male gonads and testis of adult flies (Vardanyan et al., 2008). Targeted gene disruption of DPY-30L2 leads to male sterility, sperm with impaired motility and failure to accumulate sperm in storage organs of females. In these multi-cellular organisms, various DPY-30-domain containing protein may be instrumental in forming the dimeric core for various molecular complexes.

Once tethered to modulatory moieties, such as EF hands or CaMB domains, these molecules may gain the ability to modulate structural complexes. This scenario is exemplified by *Chlamydomonas* RSP2 and a few RIIa-containing molecules. Notably, most of them are enriched in sperm flagella and ciliated tissues (Yang and Yang, 2006). They may assemble and regulate the cytoskeletal complexes in axonemes and the surrounding fibrous sheath.

The four subunits in RS, two with the DPY-30 domain and two with the RIIa domain, showcase the extraordinarily versatile applications of this superfamily. The deficiencies in *pf24* show that these two types of subunits are localized to distinct parts of the RS complex. RIIa containing RSPs (RSP11 and 7) could be targeted to the amphipathic helix in the spoke AKAP, RSP3, towards the spoke base (Gaillard et al., 2001; 2006). On the other hand, the two DPY-30 proteins (RSP2 and 23) are docked to the unknown DAP towards the spoke head and CP. Through these two distinct docking domains and respective anchoring sites, the tethered modules are precisely positioned to perform appropriate functions in the RS complex. However, none of these flagellar RIIa superfamily members have mammalian orthologs that are similar in molecular modules as well as in size. This strongly suggests that these RIIa clan family members diverge significantly. It is highly likely that these D/D domains target different effector mechanisms tailored to individual organisms.

Identification of the anchoring site for the DPY-30 domain in RSP3 will clarify this model. The RSP3 dimer may function as a scaffold protein anchoring both RIIa and DPY-30 domain containing proteins at different locations. Such a molecular arrangement explains how this important complex can physically couple moving CP and outer doublets and regulate motility as well. Together, these studies of *Chlamydomonas* radial spoke complex will ultimately reveal multiple macromolecular complexes that employ these D/D domains.

6.5 Key Findings and Significance

The *Chlamydomonas* radial spoke has been used as a system to study several concepts in ciliary and flagellar cell biology like assembly of macromolecular complexes, calcium – mediated motility response and to determine the control mechanisms of oscillatory beating. This study elucidated the importance of two proteins in the radial spoke complex (RSP2 and RSP23). These proteins have several similarities. They both share the DPY-30 domain and are calmodulin binding proteins. In addition, RSP23 has an NDK enzymatic domain. Despite their similarities, this study revealed that RSP2 and RSP23 have different functions.

- 1) The conserved N-terminus of RSP2 is important for the assembly of the RS complex.
- 2) The DPY-30 domain found in RSP2 is crucial for flagellar motility and assembly.
- 3) The calmodulin binding motif in RSP2 is required for calcium-calmodulin mediated motility response specific to *Chlamydomonas*. These regions are required only when cells are exposed to conflicting signals. This is one of the first *in vivo* studies demonstrating calcium-calmodulin mediated motility control in the radial spoke system. This result also showed that radial spokes can modulate or override phototaxis under certain conditions.
- 4) The NDK domain in RSP23 promotes flagellar assembly. This could be done by mediating assembly of several flagellar complexes. Thus its function is beyond the radial spoke complex.

This study has revealed some exciting findings that open new fields of research. The DPY-30 domain is an evolutionarily conserved domain. Proteins containing this domain

are found in several chromosome modification complexes. However, their role in these complexes has been poorly investigated. Other members of this family are not limited to the nucleus and have a broad expression profile. This suggests that the DPY-30 domain may have a common function in all these proteins. This study has shown that the DPY-30 domain (of RSP2) along with the flanking coiled coil region is important for assembly and stability of the RS complex. Based on the similarity of the DPY-30 domain to RIIa domain and the importance of DPY-30 like N-terminal sequences in Trypanosomes for targeting proteins, a model is proposed for the role of DPY-30 domain. The DPY-30 domain dimerizes and functions as a docking domain. The docking function of this domain may target the associated domain (like the coiled coil region of RSP2 or the NDK domain of RSP23) for assembly of RS or localized enzymatic activity. This explains the presence of the DPY-30 domain in different types of proteins. Several macromolecular complexes use the DPY-30 domain that can target the associated structural, enzymatic or signaling domain to the complex during its assembly. Incorporation of the DPY-30 domain protein may promote assembly of other proteins into the complex (like RSP23 and HSP40 is dependent on RSP2). This possibility can be further explored in higher organisms or other macromolecular complexes to identify DPY-30 interacting partners and the importance of such interactions.

REFERENCES

- Afzelius, B. (1976). A human syndrome caused by immotile cilia. *Science* 193, 317-319.
- Afzelius, B. (2004). Cilia-related diseases. *J Pathol* 204, 470-477.
- Almaula, N., Lu, Q., Delgado, J., Belkin, S., and Inouye, M. (1995). Nucleoside diphosphate kinase from *Escherichia coli*. *J Bacteriol* 177, 2524-2529.
- Arnold, K., Bordoli, L., Kopp, J., and Schwede, T. (2006). The SWISS-MODEL Workspace: A web-based environment for protein structure homology modelling. *Bioinformatics*, 22, 195-201.
- Badano, J., Mitsuma, N., Beales, P., and Katsanis, N. (2006). The ciliopathies: an emerging class of human genetic disorders. *Annu Rev Genomics Hum Genet* 7, 125-148.
- Barthel, T., and Walker, G. (1999). Inferences concerning the ATPase properties of DnaK and other HSP70s are affected by the ADP kinase activity of copurifying nucleoside-diphosphate kinase. *J Biol Chem* 274, 36670-36678.
- Bessen, M., Fay, R., and Witman, G. (1980). Calcium control of waveform in isolated flagellar axonemes of *Chlamydomonas*. *J Cell Biol* 86, 446-455.
- Bloch, M., and Johnson, K. (1995). Identification of a molecular chaperone in the eukaryotic flagellum and its localization to the site of microtubule assembly. *J Cell Sci* 108 (Pt 11), 3541-3545.
- Brokaw, C. (1982). Introduction: generation of the bending cycle in cilia and flagella. *Prog Clin Biol Res* 80, 137-141.
- Brokaw, C., and Luck, D. (1983). Bending patterns of *Chlamydomonas* flagella I. Wild-type bending patterns. *Cell Motil* 3, 131-150.
- Casey, D., Yagi, T., Kamiya, R., and Witman, G. (2003). DC3, the smallest subunit of the *Chlamydomonas* flagellar outer dynein arm-docking complex, is a redox-sensitive calcium-binding protein. *J Biol Chem* 278, 42652-42659.
- Castleman, V., Romio, L., Chodhari, R., Hirst, R., de Castro, S., Parker, K., Ybot-Gonzalez, P., Emes, R., Wilson, S., Wallis, C. et al. (2009). Mutations in radial spoke head protein genes RSPH9 and RSPH4A cause primary ciliary dyskinesia with central-microtubular-pair abnormalities. *Am J Hum Genet* 84, 197-209.
- Cho, Y., Hong, T., Hong, S., Guo, H., Yu, H., Kim, D., Guszczynski, T., Dressler, G., Copeland, T., Kalkum, M., and Ge, K. (2007). PTIP associates with MLL3- and MLL4-containing histone H3 lysine 4 methyltransferase complex. *J Biol Chem* 282, 20395-20406.

- Chuang, P., Lieb, J., and Meyer, B. (1996). Sex-specific assembly of a dosage compensation complex on the nematode X chromosome. *Science* 274, 1736-1739.
- Chuma, S., Hiyoshi, M., Yamamoto, A., Hosokawa, M., Takamune, K., and Nakatsuji, N. (2003). Mouse Tudor Repeat-1 (MTR-1) is a novel component of chromatoid bodies/nuages in male germ cells and forms a complex with snRNPs. *Mech Dev* 120, 979-990.
- Coba, M., Pocklington, A., Collins, M., Kopanitsa, M., Uren, R., Swamy, S., Croning, M., Choudhary, J., and Grant, S. (2009). Neurotransmitters drive combinatorial multistate postsynaptic density networks. *Sci Signal* 2, ra19.
- Cole, D.G., Diener, D.R., Himelblau, A.L., Beech, P.L., Fuster, J.C., and Rosenbaum, J.L. (1998). *Chlamydomonas* kinesin-II-dependent intraflagellar transport (IFT): IFT particles contain proteins required for ciliary assembly in *Caenorhabditis elegans* sensory neurons. *J Cell Biol* 141, 993-1008.
- Crenshaw H. C. (1993). Orientation by helical motion—I. Kinematics of the helical motion of organisms with up to six degrees of freedom. *Bull. Math. Biol.* 55 (1): 197-212.
- DeLano, W.L. The PyMOL Molecular Graphics System (2002) DeLano Scientific, San Carlos, CA, USA. <http://www.pymol.org>.
- Diener, D., Ang, L., and Rosenbaum, J. (1993). Assembly of flagellar radial spoke proteins in *Chlamydomonas*: identification of the axoneme binding domain of radial spoke protein 3. *J Cell Biol* 123, 183-190.
- DiPetrillo, C., and Smith, E. (2010). Pcdp1 is a central apparatus protein that binds Ca(2+)-calmodulin and regulates ciliary motility. *J Cell Biol* 189, 601-612.
- Dong, X., Peng, Y., Xu, F., He, X., Wang, F., Peng, X., Qiang, B., Yuan, J., and Rao, Z. (2005). Characterization and crystallization of human DPY-30-like protein, an essential component of dosage compensation complex. *Biochim Biophys Acta* 1753, 257-262.
- Donnelly, M., Zhou, M., Millard, C., Clancy, S., Stols, L., Eschenfeldt, W., Collart, F., and Joachimiak, A. (2006). An expression vector tailored for large-scale, high-throughput purification of recombinant proteins. *Protein Expr Purif* 47, 446-454.
- Dumas, C., Lascu, I., Moréra, S., Glaser, P., Fourme, R., Wallet, V., Lacombe, M., Véron, M., and Janin, J. (1992). X-ray structure of nucleoside diphosphate kinase. *EMBO J* 11, 3203-3208.
- Friedrich, B., and Jülicher, F. (2007). Chemotaxis of sperm cells. *Proc Natl Acad Sci U S A* 104, 13256-13261.

- Fujiu, K., Nakayama, Y., Yanagisawa, A., Sokabe, M., and Yoshimura, K. (2009). *Chlamydomonas* CAV2 encodes a voltage- dependent calcium channel required for the flagellar waveform conversion. *Curr Biol* 19, 133-139.
- Gaillard, A., Diener, D., Rosenbaum, J., and Sale, W. (2001). Flagellar radial spoke protein 3 is an A-kinase anchoring protein (AKAP). *J Cell Biol* 153, 443-448.
- Gaillard, A., Fox, L., Rhea, J., Craige, B., and Sale, W. (2006). Disruption of the A-kinase anchoring domain in flagellar radial spoke protein 3 results in unregulated axonemal cAMP-dependent protein kinase activity and abnormal flagellar motility. *Mol Biol Cell* 17, 2626-2635.
- Ginger, M.L., Portman, N., and McKean, P.G. (2008). Swimming with protists: perception, motility and flagellum assembly. *Nat Rev Microbiol* 6, 838-850.
- Gold, M., Lygren, B., Dokurno, P., Hoshi, N., McConnachie, G., Taskén, K., Carlson, C., Scott, J., and Barford, D. (2006). Molecular basis of AKAP specificity for PKA regulatory subunits. *Mol Cell* 24, 383-395.
- Goodenough, U., and Heuser, J. (1985). Substructure of inner dynein arms, radial spokes, and the central pair/projection complex of cilia and flagella. *J Cell Biol* 100, 2008-2018.
- Habermacher, G., and Sale, W. (1997). Regulation of flagellar dynein by phosphorylation of a 138-kD inner arm dynein intermediate chain. *J Cell Biol* 136, 167-176.
- Harris, E. H. (1988). *The Chlamydomonas Sourcebook*, San Diego: Academic Press.
- Hsu, D., Chuang, P., and Meyer, B. (1995). DPY-30, a nuclear protein essential early in embryogenesis for *Caenorhabditis elegans* dosage compensation. *Development* 121, 3323-3334.
- Huang, B., Piperno, G., Ramanis, Z., and Luck, D. (1981). Radial spokes of *Chlamydomonas* flagella: genetic analysis of assembly and function. *J Cell Biol* 88, 80-88.
- Hyams, J., and Borisy, G. (1978). Isolated flagellar apparatus of *Chlamydomonas*: characterization of forward swimming and alteration of waveform and reversal of motion by calcium ions in vitro. *J Cell Sci* 33, 235-253.
- Iomini, C., Li, L., Mo, W., Dutcher, S., and Piperno, G. (2006). Two flagellar genes, AGG2 and AGG3, mediate orientation to light in *Chlamydomonas*. *Curr Biol* 16, 1147-1153.
- Johnson, K. (1995). Immunoelectron microscopy. *Methods Cell Biol* 47, 153-162.

- Johnson, K., and Rosenbaum, J. (1992). Polarity of flagellar assembly in *Chlamydomonas*. *J Cell Biol* 119, 1605-1611.
- Kamiya, R. (2002). Functional diversity of axonemal dyneins as studied in *Chlamydomonas* mutants. *Int Rev Cytol* 219, 115-155.
- Kamiya, R., and Witman, G. (1984). Submicromolar levels of calcium control the balance of beating between the two flagella in demembrated models of *Chlamydomonas*. *J Cell Biol* 98, 97-107.
- Kaup, U., Kashikar, N., and Weyand, I. (2008). Mechanisms of sperm chemotaxis. *Annu Rev Physiol* 70, 93-117.
- King, S., and Dutcher, S. (1997). Phosphoregulation of an inner dynein arm complex in *Chlamydomonas reinhardtii* is altered in phototactic mutant strains. *J Cell Biol* 136, 177-191.
- Kozminski, K.G., Johnson, K.A., Forscher, P., and Rosenbaum, J.L. (1993). A motility in the eukaryotic flagellum unrelated to flagellar beating. *Proc Natl Acad Sci U S A* 90, 5519-5523.
- Lacombe, M., Milon, L., Munier, A., Mehus, J., and Lambeth, D. (2000). The human Nm23/nucleoside diphosphate kinases. *J Bioenerg Biomembr* 32, 247-258.
- Larkin, M.A., Blackshields, G., Brown, N.P., Chenna, R., McGettigan, P.A., McWilliam, H., Valentin, F., Wallace, I.M., Wilm, A., Lopez, R., Thompson, J.D., Gibson, T.J. and Higgins, D.G. (2007). ClustalW and ClustalX version 2. *Bioinformatics* 23(21): 2947-2948.
- Lascu, L., Giartosio, A., Ransac, S., and Erent, M. (2000). Quaternary structure of nucleoside diphosphate kinases. *J Bioenerg Biomembr* 32, 227-236.
- Leung, S., and Hightower, L. (1997). A 16-kDa protein functions as a new regulatory protein for Hsc70 molecular chaperone and is identified as a member of the Nm23/nucleoside diphosphate kinase family. *J Biol Chem* 272, 2607-2614.
- Li, J., Gerdes, J., Haycraft, C., Fan, Y., Teslovich, T., May-Simera, H., Li, H., Blacque, O., Li, L., Leitch, C. et al. (2004). Comparative genomics identifies a flagellar and basal body proteome that includes the BBS5 human disease gene. *Cell* 117, 541-552.
- Lieb, J., Capowski, E., Meneely, P., and Meyer, B. (1996). DPY-26, a link between dosage compensation and meiotic chromosome segregation in the nematode. *Science* 274, 1732-1736.
- Lombardi, D., Lacombe, M., and Paggi, M. (2000). nm23: unraveling its biological function in cell differentiation. *J Cell Physiol* 182, 144-149.

- Luck, D., Piperno, G., Ramanis, Z., and Huang, B. (1977). Flagellar mutants of *Chlamydomonas*: studies of radial spoke-defective strains by dikaryon and revertant analysis. *Proc Natl Acad Sci U S A* 74, 3456-3460.
- Lupas, A., Van Dyke, M., and Stock, J. (1991). Predicting Coiled Coils from Protein Sequences, *Science* 252:1162-1164.
- Merchant, S., Prochnik, S., Vallon, O., Harris, E., Karpowicz, S., Witman, G., Terry, A., Salamov, A., Fritz-Laylin, L., Maréchal-Drouard, L. et al. (2007). The *Chlamydomonas* genome reveals the evolution of key animal and plant functions. *Science* 318, 245-250.
- Mitchell, B., Pedersen, L., Feely, M., Rosenbaum, J., and Mitchell, D. (2005). ATP production in *Chlamydomonas reinhardtii* flagella by glycolytic enzymes. *Mol Biol Cell* 16, 4509-4518.
- Moss, A., Pazour, G., and Witman, G. (1995). Assay of *Chlamydomonas* phototaxis. *Methods Cell Biol* 47, 281-287.
- Munier, A., Feral, C., Milon, L., Pinon, V., Gyapay, G., Capeau, J., Guellaen, G., and Lacombe, M. (1998). A new human nm23 homologue (nm23-H5) specifically expressed in testis germinal cells. *FEBS Lett* 434, 289-294.
- Munier, A., Serres, C., Kann, M., Boissan, M., Lesaffre, C., Capeau, J., Fouquet, J., and Lacombe, M. (2003). Nm23/NDP kinases in human male germ cells: role in spermiogenesis and sperm motility? *Exp Cell Res* 289, 295-306.
- Nagy, P., Griesenbeck, J., Kornberg, R., and Cleary, M. (2002). A trithorax-group complex purified from *Saccharomyces cerevisiae* is required for methylation of histone H3. *Proc Natl Acad Sci U S A* 99, 90-94.
- Nonaka, S., Shiratori, H., Saijoh, Y., and Hamada, H. (2002). Determination of left-right patterning of the mouse embryo by artificial nodal flow. *Nature* 418, 96-99.
- Ogawa, K., and Gibbons, I. (1976). Dynein 2. A new adenosine triphosphatase from sea urchin sperm flagella. *J Biol Chem* 251, 5793-5801.
- Okita, N., Isogai, N., Hirono, M., Kamiya, R., and Yoshimura, K. (2005). Phototactic activity in *Chlamydomonas* 'non-phototactic' mutants deficient in Ca²⁺-dependent control of flagellar dominance or in inner-arm dynein. *J Cell Sci* 118, 529-537.
- Omoto, C., and Kung, C. (1979). The pair of central tubules rotates during ciliary beat in *Paramecium*. *Nature* 279, 532-534.
- Omoto, C.K., Gibbons, I.R., Kamiya, R., Shingyoji, C., Takahashi, K., and Witman, G.B. (1999). Rotation of the central pair microtubules in eukaryotic flagella. *Mol Biol Cell* 10, 1-4.

Patel-King, R., Gorbatyuk, O., Takebe, S., and King, S. (2004). Flagellar radial spokes contain a Ca²⁺-stimulated nucleoside diphosphate kinase. *Mol Biol Cell* 15, 3891-3902.

Pazour, G., Agrin, N., Leszyk, J., and Witman, G. (2005). Proteomic analysis of a eukaryotic cilium. *J Cell Biol* 170, 103-113.

Piperno, G., Huang, B., and Luck, D. (1977). Two-dimensional analysis of flagellar proteins from wild-type and paralyzed mutants of *Chlamydomonas reinhardtii*. *Proc Natl Acad Sci U S A* 74, 1600-1604.

Piperno, G., Ramanis, Z., Smith, E.F. and Sale, W.S. (1990). Three distinct inner dynein arms in *Chlamydomonas* flagella: molecular composition and location in the axoneme. *J. Cell Biol.* 110:379-389.

Porter, M., and Sale, W. (2000). The 9 + 2 axoneme anchors multiple inner arm dyneins and a network of kinases and phosphatases that control motility. *J Cell Biol* 151, F37-42.

Prakash, S., Tian, L., Ratliff, K., Lehotzky, R., and Matouschek, A. (2004). An unstructured initiation site is required for efficient proteasome-mediated degradation. *Nat Struct Mol Biol* 11, 830-837.

Pullen, T., Ginger, M., Gaskell, S., and Gull, K. (2004). Protein targeting of an unusual, evolutionarily conserved adenylate kinase to a eukaryotic flagellum. *Mol Biol Cell* 15, 3257-3265.

Qin, H., Diener, D., Geimer, S., Cole, D., and Rosenbaum, J. (2004). Intraflagellar transport (IFT) cargo: IFT transports flagellar precursors to the tip and turnover products to the cell body. *J Cell Biol* 164, 255-266.

Rosenbaum, J., and Witman, G. (2002). Intraflagellar transport. *Nat Rev Mol Cell Biol* 3, 813-825.

Rüffer U. and Nultsch W. (1985). High-speed cinematographic analysis of the movement of *Chlamydomonas*. *Cell Motil. Cytoskeleton.* 5 (3): 251 – 263.

Sakato, M., Sakakibara, H., and King, S. (2007). *Chlamydomonas* outer arm dynein alters conformation in response to Ca²⁺. *Mol Biol Cell* 18, 3620-3634.

Sanderson, M., and Sleight, M. (1981). Ciliary activity of cultured rabbit tracheal epithelium: beat pattern and metachrony. *J Cell Sci* 47, 331-347.

Satir, P., and Sleight, M. (1990). The physiology of cilia and mucociliary interactions. *Annu Rev Physiol* 52, 137-155.

Schmidt, J., and Eckert, R. (1976). Calcium couples flagellar reversal to photostimulation

in *Chlamydomonas reinhardtii*. *Nature* 262, 713-715.

Schultz, J., Milpetz, F., Bork, P. and Ponting, C.P. (1998). SMART, a simple modular architecture research tool: Identification of signaling domains. *PNAS* 95: 5857-5864.

Scott, J. (2006). Compartmentalized cAMP signalling: a personal perspective. *Biochem Soc Trans* 34, 465-467.

Shimogawara, K., Fujiwara, S., Grossman, A., and Usuda, H. (1998). High-efficiency transformation of *Chlamydomonas reinhardtii* by electroporation. *Genetics* 148, 1821-1828.

Silflow, C., and Lefebvre, P. (2001). Assembly and motility of eukaryotic cilia and flagella. Lessons from *Chlamydomonas reinhardtii*. *Plant Physiol* 127, 1500-1507.

Sizova, I., Fuhrmann, M., and Hegemann, P. (2001). A *Streptomyces rimosus* aphVIII gene coding for a new type phosphotransferase provides stable antibiotic resistance to *Chlamydomonas reinhardtii*. *Gene* 277, 221-229.

Smith, E., and Yang, P. (2004). The radial spokes and central apparatus: mechano-chemical transducers that regulate flagellar motility. *Cell Motil Cytoskeleton* 57, 8-17.

Smyth, R., and Berg, H. (1982). Change in flagellar beat frequency of *Chlamydomonas* in response to light. *Prog Clin Biol Res* 80, 211-215.

South, P., Fingerman, I., Mersman, D., Du, H., and Briggs, S. (2010). A conserved interaction between the SDI domain of Bre2 and the Dpy-30 domain of Sdc1 is required for histone methylation and gene expression. *J Biol Chem* 285, 595-607.

Tiwari, S., Kishan, K., Chakrabarti, T., and Chakraborti, P. (2004). Amino acid residues involved in autophosphorylation and phosphotransfer activities are distinct in nucleoside diphosphate kinase from *Mycobacterium tuberculosis*. *J Biol Chem* 279, 43595-43603.

Vardanyan, A., Atanesyan, L., Egli, D., Raja, S., Steinmann-Zwicky, M., Renkawitz-Pohl, R., Georgiev, O., and Schaffner, W. (2008). Dumpy-30 family members as determinants of male fertility and interaction partners of metal-responsive transcription factor 1 (MTF-1) in *Drosophila*. *BMC Dev Biol* 8, 68.

Wakabayashi, K., Ide, T., and Kamiya, R. (2009). Calcium-dependent flagellar motility activation in *Chlamydomonas reinhardtii* in response to mechanical agitation. *Cell Motil Cytoskeleton* 66, 736-742.

Wang, P., Chen, T., Luo, W., Zheng, J., Qian, R., Tanzer, M., Colley, K. and Verte, B. (1999). Immunolocalization of 6xHis-tagged proteins in CHO cells with QIAexpress® Anti-His Antibodies. *Qiagen news*. 1:3-6

- Wang, X., Lou, Z., Dong, X., Yang, W., Peng, Y., Yin, B., Gong, Y., Yuan, J., Zhou, W., Bartlam, M., Peng, X., and Rao, Z. (2009). Crystal structure of the C-terminal domain of human DPY-30-like protein: A component of the histone methyltransferase complex. *J Mol Biol* 390, 530-537.
- Wargo, M., Dymek, E., and Smith, E. (2005). Calmodulin and PF6 are components of a complex that localizes to the C1 microtubule of the flagellar central apparatus. *J Cell Sci* 118, 4655-4665.
- Warner, F., and Satir, P. (1974). The structural basis of ciliary bend formation. Radial spoke positional changes accompanying microtubule sliding. *J Cell Biol* 63, 35-63.
- Wei, M., Sivadas, P., Owen, H., Mitchell, D., and Yang, P. (2010). *Chlamydomonas* mutants display reversible deficiencies in flagellar beating and axonemal assembly. *Cytoskeleton (Hoboken)* 67, 71-80.
- Wilson, P.D., and Goilav, B. (2007). Cystic disease of the kidney. *Annu Rev Pathol* 2, 341-368.
- Wirschell, M., Pazour, G., Yoda, A., Hirono, M., Kamiya, R., and Witman, G. (2004). Oda5p, a novel axonemal protein required for assembly of the outer dynein arm and an associated adenylate kinase. *Mol Biol Cell* 15, 2729-2741.
- Wirschell, M., Zhao, F., Yang, C., Yang, P., Diener, D., Gaillard, A., Rosenbaum, J., and Sale, W. (2008). Building a radial spoke: flagellar radial spoke protein 3 (RSP3) is a dimer. *Cell Motil Cytoskeleton* 65, 238-248.
- Witman, G. (1986). Isolation of *Chlamydomonas* flagella and flagellar axonemes. *Methods Enzymol* 134, 280-290.
- Witman, G.B., and Minervini, N. (1982). Role of calmodulin in the flagellar axoneme: effect of phenothiazines on reactivated axonemes of *Chlamydomonas*. *Prog Clin Biol Res* 80, 199-204.
- Xu, Z., Gong, Q., Xia, B., Groves, B., Zimmermann, M., Mugler, C., Mu, D., Matsumoto, B., Seaman, M., and Ma, D. (2009). A role of histone H3 lysine 4 methyltransferase components in endosomal trafficking. *J Cell Biol* 186, 343-353.
- Yang, C., Compton, M., and Yang, P. (2005). Dimeric novel HSP40 is incorporated into the radial spoke complex during the assembly process in flagella. *Mol Biol Cell* 16, 637-648.
- Yang, C., Owen, H., and Yang, P. (2008). Dimeric heat shock protein 40 binds radial spokes for generating coupled power strokes and recovery strokes of 9 + 2 flagella. *J Cell Biol* 180, 403-415.

- Yang, C., and Yang, P. (2006). The flagellar motility of *Chlamydomonas* pf25 mutant lacking an AKAP-binding protein is overtly sensitive to medium conditions. *Mol Biol Cell* 17, 227-238.
- Yang, P., Diener, D., Rosenbaum, J., and Sale, W. (2001). Localization of calmodulin and dynein light chain LC8 in flagellar radial spokes. *J Cell Biol* 153, 1315-1326.
- Yang, P., Diener, D., Yang, C., Kohno, T., Pazour, G., Dienes, J., Agrin, N., King, S., Sale, W., Kamiya, R., Rosenbaum, J., and Witman, G. (2006). Radial spoke proteins of *Chlamydomonas* flagella. *J Cell Sci* 119, 1165-1174.
- Yang, P., Yang, C., and Sale, W. (2004). Flagellar radial spoke protein 2 is a calmodulin binding protein required for motility in *Chlamydomonas reinhardtii*. *Eukaryot Cell* 3, 72-81.
- Yang, P., Yang, C., Wirschell, M., and Davis, S. (2009). Novel LC8 mutations have disparate effects on the assembly and stability of flagellar complexes. *J Biol Chem* 284, 31412-31421.
- Yokoyama, R., O'toole, E., Ghosh, S., and Mitchell, D. (2004). Regulation of flagellar dynein activity by a central pair kinesin. *Proc Natl Acad Sci U S A* 101, 17398-17403.
- Zhang, H., and Mitchell, D. (2004). Cpc1, a *Chlamydomonas* central pair protein with an adenylate kinase domain. *J Cell Sci* 117, 4179-4188.